Ultrasound in Medicine & Biology 50 (2024) 317–331

Contents lists available at ScienceDirect

Ultrasound in Medicine & Biology

journal homepage: www.elsevier.com/locate/ultrasmedbio

Review Article

Safety Review of Therapeutic Ultrasound for Spinal Cord Neuromodulation and Blood–Spinal Cord Barrier Opening

Rui Xu *, Bradley E. Treeby, Eleanor Martin

Department of Medical Physics and Biomedical Engineering, University College London, London, UK

ARTICLE INFO

Keywords:
Ultrasound
Spinal cord
Neuromodulation
Blood–spinal cord barrier opening
Ablation
Safety
Thresholds

New focused ultrasound spinal cord applications have emerged, particularly those improving therapeutic agent delivery to the spinal cord via blood–spinal cord barrier opening and the neuromodulation of spinal cord tracts. One hurdle in the development of these applications is safety. It may be possible to use safety trends from seminal and subsequent works in focused ultrasound to guide the development of safety guidelines for spinal cord applications. We collated data from decades of pre-clinical studies and illustrate a clear relationship between damage, time-averaged spatial peak intensity and exposure duration. This relationship suggests a thermal mechanism underlies ultrasound-induced spinal cord damage. We developed minimum and mean thresholds for damage from these pre-clinical studies. When these thresholds were plotted against the parameters used in recent pre-clinical ultrasonic spinal cord neuromodulation studies, the majority of the neuromodulation studies were near or above the minimum threshold. This suggests that a thermal neuromodulatory effect may exist for ultrasonic spinal cord neuromodulation, and that the thermal dose must be carefully controlled to avoid damage to the spinal cord. By contrast, the intensity–exposure duration threshold had no predictive value when applied to blood–spinal cord barrier opening studies that employed injected contrast agents. Most blood–spinal cord barrier opening studies observed slight to severe damage, except for small animal studies that employed an active feedback control method to limit pressures based on measured bubble oscillation behavior. The development of new focused ultrasound spinal cord applications perhaps reflects the recent success in the development of focused ultrasound brain applications, and recent work has begun on the translation of these technologies from brain to spinal cord. However, a great deal of work remains to be done, particularly with respect to developing and accepting safety standards for these applications.

Introduction

The bio-effects of ultrasound focused on the spinal cord have been studied for decades. Early investigations in the 1950s sought to understand the potential for "tractless lesioning" and damage to the spinal cord using focused ultrasound [1,2]. These studies found that sufficiently intense focused ultrasound caused paraplegia and hemorrhage in their animal models. It was also observed that certain sonication regimes led to reversible changes in reflex arcs in the spinal cord and modifications in the permeability of the blood–brain barrier, which is functionally similar to the blood–spinal cord barrier [3–5]. Despite some initial promising results, the adoption of treatments based on these bio-effects was limited by the need for invasive procedures such as craniotomies and laminectomies to gain access to the brain and spinal cord. Today, advances in treatment guidance, treatment monitoring and non-invasive trans-skull focusing methods have enabled the clinical adoption of focused ultrasound thalamotomies [6] and may enable many new ultrasonic brain therapies [7–9]. These advances suggest that the time is right for the development of focused ultrasound spinal cord therapies.

The development and clinical translation of focused ultrasound spinal cord therapies lags behind those involving the brain, possibly because there are fewer identified treatable indications or perhaps because of the added difficulty of focusing ultrasound through the spine. However, the recent emergence of exciting applications such as microbubble-mediated blood–spinal cord barrier opening (BSCBo) for improved therapeutic agent delivery to the spinal cord [10–18] and spinal cord neuromodulation [19–22] may help change this trend. These focused ultrasound spinal cord applications are still at the pre-clinical stage, and the safety of these applications must be established to move forward.

A thorough literature review was conducted to identify relevant works on the topic of focused ultrasound and the spinal cord. Google Scholar keyword searches were utilized to identify articles. Additional articles were identified through examination of citation lists and references in the initial articles found. This nested approach identified several articles that may not have been found through keyword searches with modern terminology. However, it should be noted that this literature review may not have captured all relevant works, as studies that are not

* Corresponding author. Department of Medical Physics and Biomedical Engineering, University College London, London WC1E 7JE, UK.
E-mail address: rui.xu@ucl.ac.uk (R. Xu).

https://doi.org/10.1016/j.ultrasmedbio.2023.11.007
Received 18 June 2023; Revised 7 November 2023; Accepted 10 November 2023

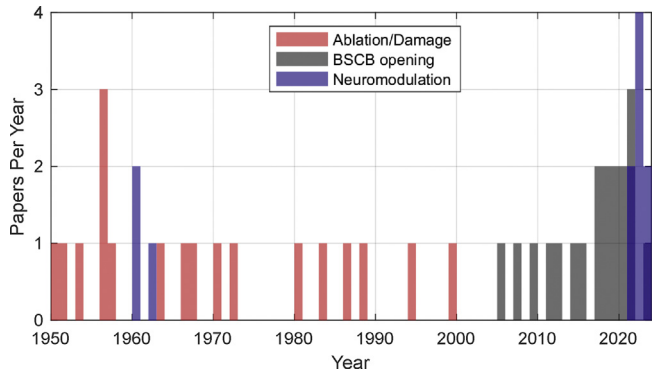

Figure 1. Number of papers published per year on ultrasound-induced spinal cord damage, blood–spinal cord barrier (BSCB) opening, and spinal cord neuromodulation from 1950 to 2023.

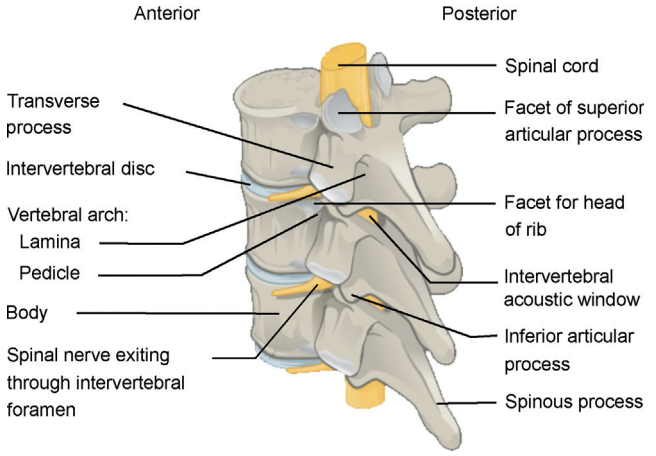

Figure 2. Thoracic spine and spinal cord illustration. Wikimedia Commons. Source: Jmarchn. Modified here. This file is licensed under the Creative Commons Attribution-Share Alike 3.0 Unported license.

cited by the works identified here may have been missed. Furthermore, this review does not include articles published in non-English scientific journals and did not consider works on physiotherapeutic ultrasound spinal applications. Despite these limitations, this review compiles the findings of 48 studies, a larger array of literature than is incorporated into modern focused ultrasound spinal cord studies. A systematic analysis on the parameters that influence spinal cord damage was then performed. The identified studies were placed into one of three categories: damage (under Ablation and Damage), neuromodulation (Section IV) and BSCBo (under Blood–Spinal Cord Barrier Opening). Figure 1 depicts the years in which the identified articles were published and the categorization of the articles within this review.

There are many ultrasound parameters that may influence the bio-effects of a focused ultrasound spinal cord application. These parameters include the source resonant frequency, the source sonication mode (*e.g.,* pulsed vs. continuous sonication, see Figure 4 for the pulse nomenclature used in this review), the source geometry, the source pressure and the resulting spatial peak pulse averaged intensity (I_{SPPA}) and spatial peak time averaged intensity (I_{SPTA}). Modifying the pre-clinical model, either by microbubble injection or by varying temperature, ambient pressure and atmospheric gas content can also lead to differences in ultrasound-induced bio-effects. Many different parameters and models have been tested in focused ultrasound spinal cord studies, which make direct comparisons between studies challenging. However, it also offers the opportunity to identify general damage trends that may be broadly applied for safety in future studies that may not exactly match the parameters of a pre-existing study. This review provides a comprehensive list of relevant parameters and tests for trends in exposure duration, intensity and resultant bio-effects. This review is written from a safety perspective; most modern neuromodulatory or BSCBo studies check for damage within their experimental groups, but their parameters are not contextualized by the many historical studies that specifically investigated ultrasound-induced spinal cord damage. The contextualization of these studies is attempted here, and it is hoped that the safety trends identified here may be applied to future studies.

Anatomy of the spine and ultrasonic considerations

Many pre-clinical models have been used to investigate the bio-effects of focused ultrasound on the spinal cord, from mouse neonates, weighing under 2 g, to juvenile pigs, weighing up to 40 kg. The use of smaller pre-clinical models can simplify a study as the spine of a small animal is less acoustically aberrating than large animal or human spines, but may affect the applicability of the study to future human trials.

The spinal cord, much like the brain, is encased in bone. A section of the human spinal cord and three thoracic vertebrae are illustrated in Figure 2. The irregular structure of the vertebrae adds different challenges (and possible opportunities) to focusing ultrasound on the spinal cord, when compared with the skull. The strong reflections at the soft tissue–bone and bone–soft tissue interfaces, along with the high attenuation rates within the bone, make it difficult to deliver ultrasound through bone. Additionally, the irregular vertebral surfaces tend not to be conducive to normal-incidence transmission, further reducing the efficiency of trans-vertebral compressional-wave ultrasound transmission from an extracorporeal source when compared with trans-skull transmission [23]. However, intervertebral acoustic windows may allow sound to pass through the spine to some spinal cord targets without being intercepted by bone. A set of experiments revealed that ultrasound transmission through ex vivo human thoracic vertebrae was approximately 30%, but varied strongly by target position [24]. Another approach to delivering ultrasound through the spine is laminectomy, a highly invasive procedure in which the spinous process and laminae of one or several vertebrae are surgically removed before the therapy. With this approach, ultrasound can reach the spinal cord without incurring pre-focal aberrations. Laminectomies are often performed even in small animal model pre-clinical studies to reduce variability in in situ intensity. However, reflections from the vertebral bodies may still generate standing waves, and pressures may exceed the free-field focal values [25]. Laminectomies are unlikely to be accepted as standard care in an ultrasound-based spinal cord therapy.

The spine is also encased in several centimeters of soft tissues, including ligaments, muscles, fat and skin. These tissues will attenuate and further aberrate focused ultrasound as it travels towards the intended target. The spinal cord resides within the spinal canal, occupying approximately 25% of the canal volume in healthy cervical spines [26]. Several meninges (from outermost to innermost: the dura mater, the arachnoid mater and the pia mater) and the space between arachnoid and pial meninges containing cerebrospinal fluid fill most of the remaining canal volume. The meninges and spinal cord are well supplied by vasculature; the spinal cord has three main arteries (two posterior arteries and one anterior artery), two main veins (one posterior vein and one anterior vein) and an extensive network of smaller vasculature within the spinal cord. The spinal cord and surrounding soft tissue structures will not influence the ultrasound intensity distribution of a focused ultrasound spinal cord therapy to the same degree as the spine, but these structures remain important to consider in terms of possible damage when evaluating the safety of an ultrasound intensity spatial distribution. High-intensity focused ultrasound can directly destroy tissues by sufficiently heating a focal area [27], and histotripsy can directly destroy tissues by generating intense acoustic cavitation from the endogenous gas in tissues [28]. Both high-intensity focused ultrasound and histotripsy have many useful applications outside of the spine, but these

treatment regimens are not discussed in this review because of the sensitivity and criticality of the spinal cord.

Ablation and damage

Early investigations into the bio-effects of ultrasound on the spinal cord revealed that focused ultrasound could produce lesions that resulted in easily measurable hindlimb paralysis. When combined, these studies appear to have had dual motivations:

1. To investigate the potential therapeutic applications of ultrasonic ablation in the spinal cord. For example, early ablation studies aimed to investigate if an ultrasound-generated focal lesion could prevent the transmission of intractable pain to the brain or prevent the transmission of dysfunctional motor signals.
2. To establish damage thresholds for exposure time (defined here as the total treatment time, inclusive of 'off' periods during pulse sonications) and intensity, to ensure the safety of ultrasound imaging sequences.

We identified 19 studies that investigated irreversible changes or damage in the spinal cord. These studies tested multiple categorical parameters, including low versus normal animal temperature, high versus normal ambient pressure, hypoxic versus normoxic atmospheres and continuous versus pulsed sonications. These studies also tested pseudo-continuous parameters including source frequency and the probability of paralysis. These parameters are characterized here as pseudo-continuous because (i) source frequency is not varied continuously in any of these studies, instead relying on using the source harmonics to efficiently generate multiple frequencies, and (ii) permanent paralysis is binary but many studies performed probit analyses [29] to identify the thresholds for 10%, 50% and 90% probability of paralysis. The identified studies also tested continuous parameters (albeit in limited ranges), including total treatment time, the non-derated mechanical index and the spatial peak pulse-averaged intensity (I_{SPPA}). The treatment time and the I_{SPPA} were used here to calculate the I_{SPTA}:

$$I_{SPPA} = I_{SPPA} \times \frac{\text{On Time}}{\text{Total Treatment Time}} \quad (1)$$

Total time and exposure time are used interchangeably throughout this text; 'on time' is the term used to describe the time with the source actively sonicating. This approach to calculating I_{SPTA} was taken to account for the cumulative thermal energy contributions of pulsed sequences with sufficiently high pulse repetition frequencies that do not allow for heat to fully dissipate away from the target tissues during the "off" times. The time over which averaging should be performed is an active question in the field; here we use the total treatment time to better align with the CEM43°C (cumulative equivalent minutes at 43°C) metric for thermal dose. Unfortunately, none of the identified studies report thermal dose or data that would enable the accurate calculation of thermal dose. I_{SPTA} values were recalculated for studies with sonications that incorporated repeated pulse trains where I_{SPTA} was calculated over the pulse repetition interval (see Figure 4). The time period limit used in this article for treatments that span multiple days was the total treatment per session where treatment-induced heating may be expected to persist. For example, the total treatment time for treatments repeated

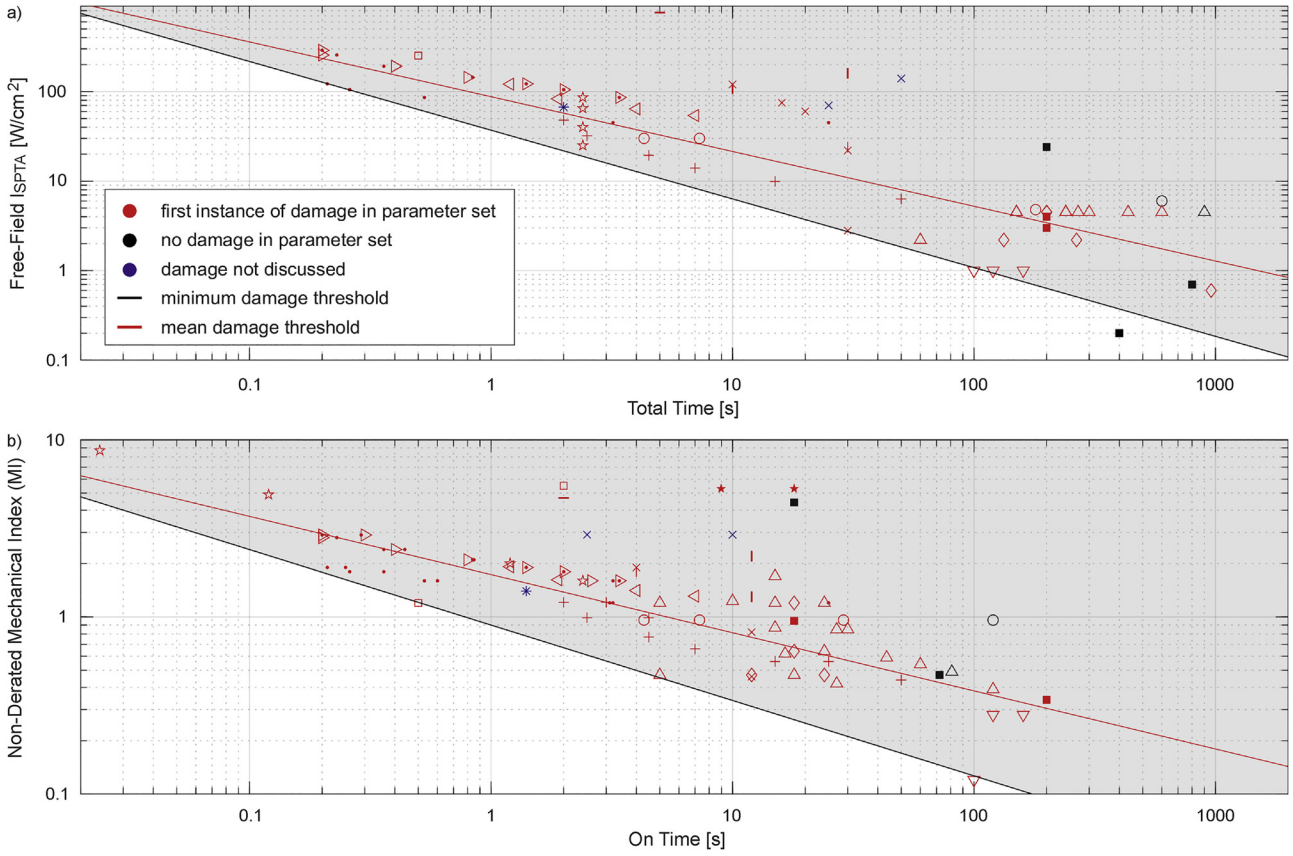

Figure 3. Earliest or lowest-intensity instance of damage in a parameter set for the identified spinal cord damage studies, plotted by (a) time-averaged spatial peak intensity (I_{SPTA}) and total treatment time and (b) non-derated mechanical index and source "on time." *Red* denotes damage, *black* denotes no damage with the given parameters and *blue* denotes parameter sets where damage was not discussed. ○, Fry et al. 1951 [1]; +, Fry et al. 1951 [2]; *, Fry and Fry 1953 [41]; ◁, Fry and Dunn 1956 [32]; ×, Hüter et al. 1956 [36]; |, Ballantine et al. 1956 [37]; −, Bowsher 1957 [38]; ★, Curry and Beaton 1958 [136]; □, Lele 1964 [137]; o, Taylor 1970 [42]; △, Taylor and Pond 1972 [43]; ▽, Stolzenberg et al. 1980 [40]; ▷, Frizell et al. 1983 [33]; •, Lee and Frizzell 1988 [31]; ☆, Frizell et al. 1994 [35]; ■, Miller et al. 1999 [39]. Curve fitting was performed to obtain the minimum thresholds (*black lines*) and mean thresholds (*red lines*) for the onset of spinal cord damage.

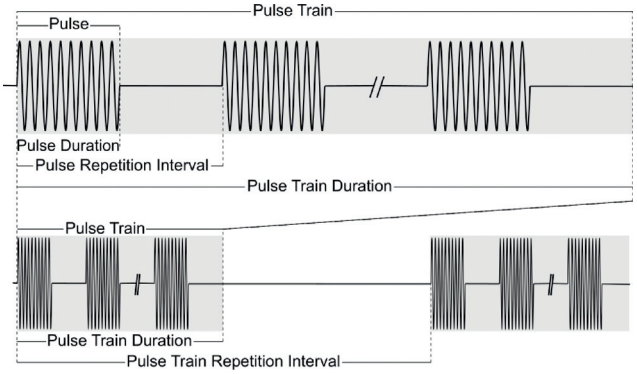

Figure 4. Pulsed sonication nomenclature used throughout this review. Pulse repetition frequency and pulse train repetition frequency are obtained from the inverses of the pulse repetition interval and the pulse train repetition interval. This review merges several pulse naming conventions.

once per day was set to the treatment time within 1 d, and the total treatment time for treatments repeated once every 12 h was set to the treatment time within each 12 h period. This time period limit may need to be revisited as the field learns more about the effects of prolonged and repetitive ultrasound exposure.

Mechanical damage to the spinal cord is parameterized in this review using the source "on time" and the non-derated mechanical index (MI), which is defined as

$$\mathrm{MI(non-derated)} = p_r/\sqrt{f_c} \tag{2}$$

where p_r is the spatial peak rarefactional pressure in water, and f_c is source centre frequency. The non-derated MI differs from the MI used in ultrasonic imaging; in the standard MI used in ultrasonic imaging, the p_r is derated by 0.3 dB/cm [30]. The non-derated MI is used here because the depths and attenuation coefficients of the intervening dorsal tissues are not known and the dorsal tissues were often modified via laminectomy and surgical exposure of the spinal cord. Here, we consistently report non-derated MI values rather than estimated derated values for each animal model. Most historical studies report intensity rather than a p_r value; when the p_r value is not reported, it is estimated from the reported intensity by assuming that the signal is linear and travelling as a plane wave. These assumptions result in some uncertainty in the MI values reported in this review, particularly in studies that implemented high intensities.

This review identifies damage thresholds for exposure time and I_{SPTA}, and the transducer "on time" and non-derated MI. Of the 19 studies identified, 16 had identifiable parameters for (or related parameters that enabled the calculation of) exposure time, "on time," I_{SPTA} and non-derated MI. The minimum exposure time or I_{SPTA} for the earliest/lowest intensity instance of damage for each tested parameter combination from each study is given in Figure 3a. Here, a "parameter combination" refers to a single frequency, a single sonication mode and a single animal model and environmental conditions, but variable intensity or exposure duration. A clear relationship can be seen between the logarithm of exposure time and the logarithm of the I_{SPTA}. A line corresponding to the minimum reported exposure damage threshold in log–log space was obtained from the four lowest I_{SPTA} values—total treatment times that underline the remainder of the Figure 3a distribution. The threshold function fitting was performed using MATLAB 2022a (The MathWorks, Natick, MA, USA) fit algorithm for an equation of the form $y = At^B$ to obtain:

$$I_{SPTA} = 37(t_{total})^{-0.77}\left[\mathrm{W/cm^2}\right] \tag{3}$$

where t_{total} is the total treatment time in seconds. Equation (3) can be used to estimate the minimum I_{SPTA} for possible damage at a given exposure time, or can be re-arranged to estimate the minimum exposure time that may result in damage at a given I_{SPTA}. The mean I_{SPTA}– exposure time threshold was obtained by fitting an equation of the same form to the earliest/lowest-intensity instance of damage reported for each tested parameter combination from each study, and the fit values are outlined in Table 1.

Table 1
Fit values for focused ultrasound-induced spinal cord damage as a function of total time and I_{SPTA} or of time and MI

Parameter	*A*	95% CI	*B*	95% CI
Min [I_{SPTA}]	37	35 to 39	−0.77	−0.81 to -0.73
Mean [I_{SPTA}]	88	73 to 103	−0.61	−0.72 to -0.51
Min [MI]	0.90	0.63 to 1.2	−0.43	−0.62 to -0.23
Mean [MI]	1.7	1.6 to 1.9	−0.33	−0.37 to -0.28

Fit equation is $y = At^B$, where y is I_{SPTA} or mechanical index and *t* is total time or on time.
I_{SPTA}, spatial-peak time-averaged intensity.

A clear relationship can also be seen between the logarithm of "on time" and the logarithm of the non-derated MI. The minimum non-derated MI–"on time" threshold for damage was obtained from the three lowest values that underline the remainder of the Figure 3b distribution. The threshold function fitting was also performed using the MATLAB fit algorithm for an equation of the form $y = At^B$, giving the minimum threshold for damage:

$$\mathrm{MI(non-derated)} = 0.90(t_{on})^{-0.43} \tag{4}$$

where t_{on} is the source on time in seconds. Equation (4) can be used to estimate the minimum non-derated MI for possible damage for a given "on time" or can be rearranged to estimate the minimum exposure time that may result in damage at a given non-derated MI. The mean non-derated MI–"on time" threshold was obtained by fitting an equation of the same form to the earliest/lowest non-derated MI instance of reported damage for each tested parameter combination. The fit values for the minimum and mean damage thresholds and the 95% confidence intervals are reported in Table 1.

The thresholds used throughout this review are based solely on the data reported from the identified studies and reveal the limits of the parameters reported across these studies in which damage was observed, to show the trends. They are not intended to be interpreted as safety thresholds below which there will be no damage or as a threshold above which damage is certain. The thresholds presented here are intended to illustrate increasing risk with increasing exposure, to facilitate comparison of studies and the planning of future studies, but they are not intended to explicitly define safe/unsafe regions of the parameter space. To do so requires the development of appropriate safety margins around the thresholds; this is not attempted here.

The non-derated MI values in the 16 identified studies are low relative to established estimated non-derated MI thresholds for cavitation [30]. A review of 13 studies found an average estimated MI threshold for cavitation of 7.2 (3.8–14.8) across various animal tissues [30], and only one study identified here exceeded this average value. The signal-linearity assumption used in this review will overestimate the p_r values of non-linear signals, in turn resulting in an overestimation of the non-derated MI values. This may place the actual non-derated MI values further below the estimated MI threshold for cavitation [30]. Mechanical effects may still damage the spinal cord at sufficiently high MI values, and there may be combined thermal and mechanical effects where heating reduces the cavitation threshold [31], resulting in cavitation-based damage later in a focused ultrasound exposure. While the in situ MI may still be a useful metric for predicting possible mechanical damage in the absence of injected contrast agents, the I_{SPTA}–time damage threshold will be prioritized in later discussion of ultrasound-induced damage in this review.

Equation 3 gives an estimate of the threshold for spinal cord damage based solely on exposure duration and I_{SPTA}, as plotted in Figure 3a.

This equation does not incorporate any adjustments for other parameters that may influence spinal cord-focused ultrasound tolerance; Figure 3a and eqn (3) include models and testing conditions that reduce the exposure intensity or duration needed to generate damage. If a planned study is to exceed the threshold described by eqn (3), then a careful comparison of the study's parameters relative to those reported here should be undertaken to understand the risks associated with the study. It is also important to note that the clear relationship between exposure time and I_{SPTA} may not persist at long exposure times and low intensities: several parameter combinations with long exposure times and lower I_{SPTA} did not result in observable spinal cord damage despite crossing the threshold defined in eqn (3). This may be because of variable heat diffusion rates and/or perfusion removing heat, preventing the spinal cord from reaching damaging temperatures.

The pre-clinical studies plotted in Figure 3 and three other studies with incomplete intensity-versus-exposure duration information are discussed in detail in Appendix S1 (online only). An accounting of the experimental subjects, average subject weights, number of subjects, target, laminectomy, sonication frequency and mode, transducer "on time," I_{SPPA}/I_{SPTA}, spinal cord heating and damage is also provided in brief in Table 2 and in greater detail in a supplementary Excel file (online only).

Although the foundational studies on focused ultrasound spinal cord bio-effects were performed in frogs [1,2], all of the following studies used mammals. The tested mammals spanned more than three orders of magnitude in body mass, beginning with neonatal mice [31–35], then mice [36–39] or pregnant mice [40], rats [41–43] and finally cats [44,45]. All studies that used rats or cats used surgical laminectomies to obtain access to the spinal cords, reducing the discrepancy between the reported free-field intensities and the in situ intensities. The studies performed in mice or frogs did not use laminectomies, but the smaller size of these animals means that the intervening tissues (spine and soft tissues) cause smaller decreases in in situ intensities relative to free-field intensities.

One parameter that was investigated in several studies was the model body temperature. This may have been partially owing to the anaesthetizing effect of low body temperatures, which allowed the researchers to easily position the animals during the experiments. Approximately half of the studies were performed with cooled animals [1,2,31–35], and the remaining studies were performed while at normal physiological temperatures [1,31,37,39,40,43–46]. Cooling the animals prior to ultrasound application increased the animal's ultrasound exposure tolerance, most likely by increasing the exposure time needed for the spinal cord to reach damaging temperatures.

Most of the identified studies were performed in a natural atmosphere [1,32,36–40,44–46], but some studies investigated hyperbaric pressures that were intended to reduce or prevent cavitation [2,31,33–35], and two studies investigated artificial atmospheres that were intended to induce hypoxia [42,43]. Hyperbaric pressures were found to have either no effect (in mouse neonates at an I_{SPTA} below 100 W/cm^2) or slightly increase the exposure tolerance (in mouse neonates at higher intensities or in frogs). The increase in exposure tolerance is attributed to the suppression of cavitation either within the animals or within the coupling medium. Gas concentrations intended to produce hypoxia resulted in lower exposure tolerance [42,43], perhaps because hypoxia alone can be damaging to neurons [47].

The studies that lie along the minimum threshold for damage illustrated in Figure 3a and defined in eqn (3) are:

- The very high-intensity (an I_{SPPA} of approximately 2000 W/cm^2) 1 MHz pulsed wave 10°C mouse neonate experiment [35].
- The high-intensity (an I_{SPTA} of approximately 100 W/cm^2) 1 MHz continuous wave 37°C mouse neonate experiments [31].
- The relatively low-intensity (an I_{SATA} of approximately 2.8 W/cm^2) pulsed wave 1 MHz mouse experiment [36]. Here, intensity was given as a spatial average instead of a spatial peak value and the corresponding I_{SPTA} value would lie above the minimum threshold. However, the authors reported a 50% probability of paralysis at the given I_{SATA}, meaning that the threshold for, for example, 5% paralysis, would be lower than the given I_{SATA} value lie below the minimum threshold. These attributes oppose each other.
- The pregnant mouse experiment performed at low intensity (an I_{SPTA} of 1 W/cm^2) with pulsed or continuous 2 MHz sonications with a large-beam-area unfocused source that also caused off-target effects such as lung haemorrhage [40].

It is important to note that the values reported for two of the studies that form eqn (3) are for 10% paralysis within a group [31,35] and were obtained via probit analysis. It is therefore possible that paralysis could occur at lower exposures; this is a weakness of the probit analysis reporting method. The onset of paralysis likelihood is often rapid, with a factor of 2–3 separating 10% paralysis and 90% paralysis. This could suggest that 0% paralysis occurs near 10% paralysis, but this review will not speculate or attempt to extrapolate the probit analyses to 0% paralysis; uncertainty must remain in these thresholds because of individual differences and differences in sonication protocols.

The minimum damage threshold (eqn 3) includes both neonatal and adult mice, and susceptibility to ultrasound-induced spinal cord damage may depend on body mass and development stage. For example, mouse neonates have a total body mass less than 2 g, giving them very little thermal inertia and perfusive capacity. Mice are known to be less heat tolerant than larger animals and humans from experiments that have tested thermal exposure thresholds in non-spinal cord tissues (*e.g.,* skin) [48]. The difference in threshold between mice and in vivo human tissue has been estimated at between 0.5°C and 5°C [48]. The data points in Figure 3 for rats and cats are two- to threefold higher than those for mice (see Supplementary Material, online only), but the tested I_{SPTA} and total treatment time ranges differ across animal models, so there is insufficient data to determine model-specific thresholds. Future studies should perhaps treat the minimum damage threshold (eqn 3) as a guideline that they should stay below whenever possible, and above which greater caution must be applied and a case be made supporting the treatment safety. The mean damage threshold (parameters in Table 1) should not be exceeded for a non-ablative treatment without extensive evidence (*e.g.,* measurements and/or simulations that demonstrate sufficient derating of the ultrasound exposure along the beam path) that the treatment deviates from the sonications illustrated in Figure 3. Appropriate treatment monitoring methods should also be implemented across the I_{SPTA}–total treatment time range.

The analysis illustrated in Figure 3 and eqns (3) and (4) is limited to pre-clinical models. A hypothetical future in-human trial of a therapeutic focused ultrasound spinal cord application must also rely on pre-clinical experiences as there are (thankfully) no published studies or case reports discussing ultrasound-induced damage to the human spinal cord. However, many studies have investigated ultrasonic damage thresholds in the human brain, particularly in the development of thalamotomies [6], blood–brain barrier opening [7–9,49] and brain neuromodulation [50]. Only one of the identified studies investigated the intensity and exposure duration needed to generate a lesion or paralysis in both the spinal cord and the brain (in separate animal models) [37], finding that the intensity and corresponding exposure duration were similar for brain and spinal cord. The development of intensity-versus-exposure thresholds for brain continued, creating damage thresholds to similar that illustrated in Figure 3a). For example, in the Dunn and Fry plot the damage threshold for embryonic and adult central nervous system tissue at 1 MHz and 37°C for 0.1–8 s, the embryonic threshold function matches the spinal cord threshold in Figure 3a) closely, while the threshold intensity for a given exposure time in adult central nervous system tissue at 1–6 MHz was nearly an order of magnitude higher [51]. This increase in exposure threshold may result from the increase in animal body mass and perfusive capacity or the maturation of the vasculature; the underlying reason for the sensitivity of embryonic tissue is not described.

Table 2
Pre-clinical focused ultrasound spinal cord damage studies

Reference	Subject	n	Frequency	Mode	Time	I_{SPPA}	I_{SPTA}	ΔT	Damage
Fry et al. 1950 [1]	Frog	12	0.98	Continuous	?	30–40	30–40	10–30	Above 4.3 s
	Frog (1°C)	50	0.98	Continuous	?	30–40	30–40	15	Above 7.3 s
	Frog	5	0.98	0.08 s, 2 Hz	180 s	30–40	4.8–6.4	12–14	At 180 s
	Frog	5	0.98	0.01 s, 20 Hz	600 s	30–40	6.0–8.0	16–18	No
Fry et al. 1951 [2]	Frog (1°C)	5	0.98	Continuous	?	6.3	6.3	?	Above 50 s
	Frog (1°C)	5	0.98	Continuous	?	9.9	9.9	?	Above 15 s
	Frog (1°C)	5	0.98	Continuous	?	14	14	?	Above 7 s
	Frog (1°C)	10	0.98	Continuous	?	19.4	19.4	?	Above 4.5 s
	Frog (1°C)	10	0.98	Continuous	?	32	32	?	Above 2.5 s
	Frog (1°C)	10	0.98	Continuous	?	48	48	?	Above 2 s
	Frog (1°C, 13 atm)	5	0.98	Continuous	?	9.9	9.9	?	Above 25 s
	Frog (1°C, 13 atm)	10	0.98	Continuous	?	32	32	?	Above 4.5 s
	Frog (1°C, 13 atm)	10	0.98	Continuous	?	48	48	?	Above 3 s
Fry 1953 [46]	Rat (lam.)	6	0.98	Continuous	2 s	67	67	6–18	?
Fry & Dunn 1956 [32]	Mouse (24 h, 10°C)	30	0.98	Continuous	7 s	54	54	16.5	10%
	Mouse (24 h, 10°C)	30	0.98	Continuous	4 s	64	64	9	10%
	Mouse (24 h, 10°C)	100	0.98	Continuous	1.9 s	83	83	8	10%
	Mouse (24 h, 10°C)	30	0.98	Continuous	1.2 s	121	121	6	10%
Hüter 1956 [36]	Mouse	40	1	0.4 s, 1 Hz	30 s	7	2.8	?	50%
	Mouse	20	2.5	0.4 s, 1 Hz	10–60 s	55	222	?	50% at 30 s
	Mouse	20	2.5	0.1 s, 2 Hz	20 s	300	60	?	15%
	Mouse	20	2.5	0.1 s, 2.5 Hz	16 s	300	75	?	50%
	Mouse	20	2.5	0.1 s, 4 Hz	10 s	300	120	?	80%
	Mouse	20	2.5	0.4 s, 1 Hz	10 s	300	120	?	90%
	Mouse	20	2.5	1 s, 0.4 Hz	10 s	300	120	?	95%
	Mouse	1	2.5	0.1 s, 2 Hz	50 s	700	140	?12	?
	Mouse	1	2.5	0.4 s, 1 Hz	30 s	7	2.8	?8	?
Ballantine et al. 1956 [37]	Mouse	?	1	0.4 s, 1 Hz	30 s	60–200	24–80	?	30%–80%
	Mouse	?	2.5	0.4 s, 1 Hz	30 s	400–1000	160–400	?	30%–80%
	Mouse	30	2.5	0.4 s, 1 Hz	10 s	270	108	?	6%
	Mouse	30	2.5	0.4 s, 1 Hz	10 s	450	192	?	11%
	Mouse	30	2.5	0.4 s, 1 Hz	10 s	510	204	?	20%
	Mouse	30	2.5	0.4 s, 1 Hz	10 s	600	240	?	15%
	Mouse	30	2.5	0.4 s, 1 Hz	10 s	720	288	?	44%
	Mouse	30	2.5	0.4 s, 1 Hz	10 s	930	372	?	63%
	Mouse	30	2.5	0.4 s, 1 Hz	10 s	1120	448	?	78%
	Mouse	30	2.5	0.4 s, 1 Hz	10 s	1490	596	?	97%
Bowsher 1957 [38]	Mouse	10	2.5	0.4 s, 1 Hz	5 s	1900	760	?	100%
Curry & Beaton 1958 [136]	Mouse	56	2.5	0.6 s, 1 Hz	15-30 s	2200	1340	?	>20%
Richards et al. 1966 [44]	Cat (lam.)	35	2.7	0.3 s, ?Hz	?	?	?	?	Yes
Lele 1967 [45]	Cat (lam.)	Many	1, 3, 5	Continuous	0.5–2 s	252–1050	252–1050	?	Yes
Taylor 1970 [42]	Rat (lam.)	16	3.5	0.01 s, 2.5–9 Hz	180+ s	25	0.6–2.2	?	Above 24 s
	Rat (lam.)	4	3.5	0.01 s, 2.5 Hz	180+ s	50	4.5	?	Above 18 s
	Rat (lam. ↓ O_2)	8	3.5	0.01 s, 2.5 Hz	120+ s	25	2.2	?	Above 12 s
	Rat (lam.)	8	1	0.01 s, 2.5 Hz	180+ s	25	2.2	?	Above 18 s
Taylor & Pond 1972 [43]	Rat (lam.)	16	0.5	0.01 s, 9 Hz	60+ s	25–50	2.2–4.5	6	Yes
	Rat (lam.)	6	0.5	0.01 s, 9 Hz	120+ s	50	4.5	6	At 150 s
	Rat (lam. ↓ O_2)	7	0.5	0.01 s, 9 Hz	90+ s	25	2.2	?	At 100 s
	Rat (lam.)	15	1	0.01 s, 9 Hz	150+ s	50	4.5	6	At 150 s
	Rat (lam.)	6	1	0.01 s, 9 Hz	210+ s	50	4.5	6	At 240 s
	Rat (lam. ↓ O_2)	6	1	0.01 s, 9 Hz	120+ s	25	2.2	?	At 150 s
	Rat (lam.)	12	2	0.01 s, 5-9 Hz	240+ s	50	2.5-4.5	9	At 240 s
	Rat (lam.)	5	2	0.01 s, 9 Hz	240+ s	50	4.5	9	At 270 s
	Rat (lam. ↓ O_2)	6	2	0.01 s, 9 Hz	150+ s	25	2.2	?	At 160 s
	Rat (lam.)	22	3.5	0.01 s, 5–9 Hz	240+ s	25–50	1.2–4.5	10	Yes
	Rat (lam.)	6	3.5	0.01 s, 9 Hz	180+ s	50	4.5	10	At 240 s
	Rat (lam. ↓ O_2)	6	3.5	0.01 s, 9 Hz	150+ s	25	2.2	?	At 180 s
	Rat (lam.)	8	4.2	0.01 s, 9 Hz	300+ s	50	4.5	?	At 435 s
	Rat (lam. ↓ O_2)	5	4.2	0.01 s, 9 Hz	270+ s	25	2.2	?	At 270 s
	Rat (lam.)	8	4.9	0.01 s, 9 Hz	600+ s	50	4.5	?	At 600 s
	Rat (lam. ↓ O_2)	4	4.2	0.01 s, 9 Hz	1200 s	25	2.2	?	Yes
	Rat (lam.)	10	6	0.01 s, 9 Hz	900 s	50	4.5	11	No
Stolzenberg et al. 1980 [40]	Mouse (preg.)	480	2	Continuous	80+ s	1	1	?	At 100 s
	Mouse (preg.)	101	2	0.01 s, 20 Hz	80+ s	5	1	?	At 120 s
	Mouse (preg.)	88	2	0.02 s, 200 Hz	80+ s	5	1	?	At 120 s
Frizell et al. 1983 [33]	Mouse (24 h, 10°C)	>100	1	Continuous	3+ s	86	86	?	10% at 3.4 s
	Mouse (24 h, 10°C)	>100	1	Continuous	2+ s	105	105	?	10% at 2.0 s
	Mouse (24 h, 10°C)	>100	1	Continuous	1+ s	122	122	?	10% at 1.4 s
	Mouse (24 h, 10°C)	150	1	Continuous	0.8+ s	144	144	?	10% at 0.8 s
	Mouse (24 h, 10°C)	>100	1	Continuous	0.4+ s	192	192	?	10% at 0.4 s
	Mouse (24 h, 10°C)	>100	1	Continuous	0.2+ s	256	256	?	10% at 0.2 s
	Mouse (24 h, 10°C)	>100	1	Continuous	0.2+ s	289	289	?	10% at 0.2 s
Borelli et al 1986 [34]	Mouse (24 h, 10°C)	200	1	Continuous	↑	↑	↑	?	Yes

(*continued*)

Table 2 (*Continued*)

Reference	Subject	n	Frequency	Mode	Time	I_{SPPA}	I_{SPTA}	ΔT	Damage
Lee & Frizell 1988 [31]	Mouse (24 h, 10°C)	100	1	Continuous	20+ s	45	45	?	10% at 25 s
	Mouse (24 h, 10°C)	100	1	Continuous	3+ s	86	86	?	10% at 3.2 s
	Mouse (24 h, 10°C)	100	1	Continuous	2+ s	105	105	?	10% at 2 s
	Mouse (24 h, 10°C)	100	1	Continuous	1+ s	122	122	?	10% at 1.4 s
	Mouse (24 h, 10°C)	100	1	Continuous	0.8+ s	144	144	?	10% at 0.84 s
	Mouse (24 h, 10°C)	100	1	Continuous	0.3+ s	192	192	?	10% at 0.36 s
	Mouse (24 h, 10°C)	100	1	Continuous	0.2+ s	256	256	?	10% at 0.23 s
	Mouse (24 h, 10°C)	100	1	Continuous	0.2 s	289	289	?	10% at 0.2 s
	Mouse (24 h)	100	1	Continuous	3+ s	45	45	?	10% at 25 s
	Mouse (24 h)	100	1	Continuous	0.5+ s	86	86	?	10% at 0.53 s
	Mouse (24 h)	100	1	Continuous	0.2+ s	105	105	?	10% at 0.26 s
	Mouse (24 h)	100	1	Continuous	0.2+ s	122	122	?	10% at 0.21 s
Frizell et al. 1994 [35]	Mouse (24 h, 10°C)	25	1	Continuous	2.4 s	86	86	?	50% paralysis
	Mouse (24 h, 10°C)	125	1	10 μs, 50 kHz	2.4 s	130	65	?	4% paralysis
	Mouse (24 h, 10°C)	125	1	10 μs, 5 kHz	2.4 s	800	40	?	3% paralysis
	Mouse (24 h, 10°C)	125	1	10 μs, 1 kHz	2.4 s	2500	25	?	6% paralysis
Miller et al. 1999 [39]	Mouse	5	1.09	0.01 s, 9 Hz	200 s	33	3	12	↓60% grip
	Mouse	5	1.09	0.01 s, 9 Hz	800 s	8	0.7	?	↑10% grip
	Mouse	5	1.09	Continuous	200 s	4	4	?	↓70% grip
	Mouse	5	0.4	0.01 s, 9 Hz	200 s	260	24	?	ΔGrip « 0
	Mouse	5	N/A	Shockwave, 2 Hz	400 s	7500	0.1	?	ΔGrip « 0

Reported parameters include the sample size (n), frequency (MHz), total treatment time, I_{SPPA} and I_{SPTA} (both in W/cm^2), heating (ΔT, °C) and details regarding the subject (24 h denotes the age of the mice; ↓O_2 denotes a study performed under hypoxic conditions). Exposure durations in Borelli et al. [34] were obtained from Frizell et al. [33].

I_{SPPA}, spatial peak pulse averaged intensity; I_{SPTA}, spatial peak time averaged intensity; lam., laminectomy.

A direct comparison between eqn (3) and modern brain damage thresholds is difficult because modern brain damage thresholds are usually reported with CEM43°C [52], which correlates better with damage than other metrics such as intensity alone, intensity times exposure duration or peak temperature [53]. The minimum reported brain CEM43°C for damage generated by focused ultrasound, measured with magnetic resonance imaging (MRI) thermometry in a pre-clinical model is 12 min [53], but is only 7.5 min with brain heating by hot perfused blood [54]. The minimum mouse spinal cord CEM43°C for damage (heating by hot water bath or microwave, measured by thermocouple) has been reported to be approximately 20 min [48,55–57]. Unfortunately, there has yet to be a study that investigates the CEM43°C threshold for spinal cord using focused ultrasound and MRI thermometry, again making it difficult to perform a direct comparison between spinal cord and brain CEM43°C thresholds.

The identified studies present conflicting results, suggesting either that the threshold for damage is lower in the spinal cord than in brain (eqn 3 vs. Dunn and Fry [51]), that the threshold for damage is similar in brain and spinal cord [37] or that the thermal threshold for damage is higher in the spinal cord than in the brain [48,53]. Differences between studied models and ultrasonic parameters may account for the discrepancies between these studies. Future studies that use volumetric temperature measurement in a clinically relevant model subjected to a range of ultrasound intensities and exposure durations are needed to establish the brain-versus-spinal cord damage thresholds. For the time being, it seems sensible to use the most conservative argument and eqn (3) to guide choices in ultrasound parameters and exposure durations.

All of the studies discussed in this section were performed in models where the in situ ultrasound field intensity would be close to the free-field values. In mouse neonates, the ossification process is incomplete, and sound may be transmitted through the posterior elements of the spine with minimal insertion losses. In adult mice, sound may be absorbed in the posterior elements of the spine, then quickly dissipated into the spinal cord as heat because of the small size of the mouse spine, leading to spinal cord damage. In rats and cats, laminectomies were performed, allowing ultrasound to reach at least free-field intensities within the spine, or perhaps exceed the free-field values through reflections from the vertebral bodies [25]. The vertebral bodies of the rats and cats will also absorb the ultrasound, which can be dissipated back into the spinal cord as heat and cause damage. In practice, it is unlikely that laminectomies will be accepted as a component of an ultrasonic intervention, and most sound will be reflected by or absorbed within the posterior elements of the spine. Although the damage thresholds developed in this section should be helpful guidelines for implementing safe ultrasound parameters, evaluating the safety and efficacy of a potential spinal cord application will require further investigation prior to in-human experimentation.

The thresholds developed from the identified pre-clinical studies can be compared with the intensity and exposure limits given by the U.S. Food and Drug Administration (FDA), the British Medical Ultrasound Society (BMUS) and the American Institute of Ultrasound in Medicine (AIUM) for ultrasonic imaging [58,59]. The FDA ultrasound intensity limits for cephalic imaging applications are a derated I_{SPPA} <190 W/cm^2 and a derated I_{SPTA} <94 mW/cm^2, unless the thermal index is displayed, in which case the I_{SPTA} is <720 mW/cm^2 [60]. If the FDA maximum I_{SPTA} and I_{SPPA} values are inserted into eqn (3) (rearranged for t), the maximum safe pulse length according to eqn (3) is 0.12 s for the I_{SPPA} limit, and the maximum safe exposure duration is approximately 39 min at the 94 mW/cm^2 I_{SPTA} limit or 167 s at an I_{SPTA} of 720 mW/cm^2. The temporal component of eqn (3) may provide greater utility for planning pre-clinical studies than the FDA imaging limits, as it enables the calculation of intermediate threshold values that may be used to evaluate the safety of a range of intensities and exposure times. The BMUS–AIUM approach for the thermal index takes a coarse-grained approach similar to eqn (3) and sets exponentially shorter exposure time limits for increasing thermal indices. There are TI limits for cephalic applications (without skull removal, TIC) and for bone-near-focus applications (TIB); the thermal limits for adult spinal cord applications should incorporate the considerations of both thermal indices, that is, the potential for bone heating at the focus in the TIB and the potentially low thermal tolerance of spinal cord tissue in the TIC. The TI of a system is based on approximations that estimate the temperature rise at a certain power and tissue depth, but these equations may underestimate heating by a factor of 2 [58,61], are validated only for (certain) imaging sequences and incorporate several assumptions that are not be discussed at length here [62]. The TI may be a useful tool for estimating the maximum safe exposure time at a given intensity in certain applications, but a simulation of the temperature elevation resulting from a focused ultrasound spinal cord sonication could be more accurate and provide more meaningful information. Here, it is felt that current TI calculation methods do not

account for the risks of focused ultrasound spinal cord applications and should not be used to guide the safety of these applications in their current form.

The studies discussed in this section span a long period in time and experimental practices. The estimation of in situ intensities likely generates the largest source of error. Intensity was historically measured with a spherical radiometer or thermocouple calibrated with the spherical radiometer method. This method may be strongly affected by acoustic streaming at high intensities and may not be as accurate as modern hydrophone-based field characterization methods [63]. The first study in the listed spinal cord studies to use a hydrophone and report waveform traces was Frizzell et al. [35]. Despite the metrological shortcomings of some of these works, the sheer number of animals used to generate the probit analyses means the exposure thresholds are carefully defined. Summed together, nearly 5000 animals were used in the studies that form Figure 3, lending a statistical weight to this figure that would be difficult to recreate from scratch. It would be remiss of this review to exclude the historical studies because of metrological uncertainties; we should learn as much from these studies as possible.

Neuromodulation

Investigations into the neuromodulatory effects of ultrasound on the spinal cord began at a time similar to that of investigations into ultrasonic damage of the spinal cord [3,4], and there is some overlap in the early literature where several of the spinal cord damage studies observed temporary or reversible paralysis [1,33,34]. However, the "temporary/reversible" paralysis generally occurred just below the damage thresholds noted in those studies. Most of the studies discussed in this section check for the presence of damage after the neuromodulatory pulses but focus primarily on the neuromodulatory effects of the ultrasound rather than any short-term morphological changes that result from the application of ultrasound. Several studies that investigate the long-term and offline effects of focused ultrasound on the spinal cord (primarily in the context of the treatment of spinal cord injury) are cited but not discussed in detail [64–68]. The first group of online neuromodulatory studies were performed in the 1960s; then, after a multidecade gap, neuromodulatory studies involving the spinal cord emerged again in the 2020s.

Figure 5 illustrates the distribution of I_{SPTA} versus exposure time for the identified neuromodulatory studies, along with the minimum and mean exposure thresholds for damage (eqn 3) obtained from the spinal cord damage studies. An abbreviated set of the parameters implemented in the studies plotted in Figure 5 and discussed in detail in Appendix S2 (online only) are summarized in Table 3. Further details from each study are also compiled in a supplementary Excel file (online only).

The distribution of neuromodulatory study parameters falls on either side of the minimum damage threshold. This raises the following concerns:

1. The ultrasonic exposures that generate a neuromodulatory effect roughly follow the same trend as the minimum and mean damage thresholds, and the time dependence suggests a thermal mechanism.
2. Several of the studies exceed the minimum and mean damage thresholds to achieve the recorded neuromodulatory effects.

However, only two of the nine plotted studies observed damage [3,19], and in both cases the exposure parameters were well above the minimum exposure thresholds (another neuromodulatory study observed damage but did not list parameters that enable the calculation of intensity or non-derated MI [4]). Several of the other neuromodulatory studies also exceeded the minimum damage thresholds without reporting any damage, while still testing for damage. This may be owing to differences in the animal model and environment; neonatal mice and hypoxic conditions were not used in these neuromodulatory studies, and several rat studies were performed without laminectomies [19,22,69].

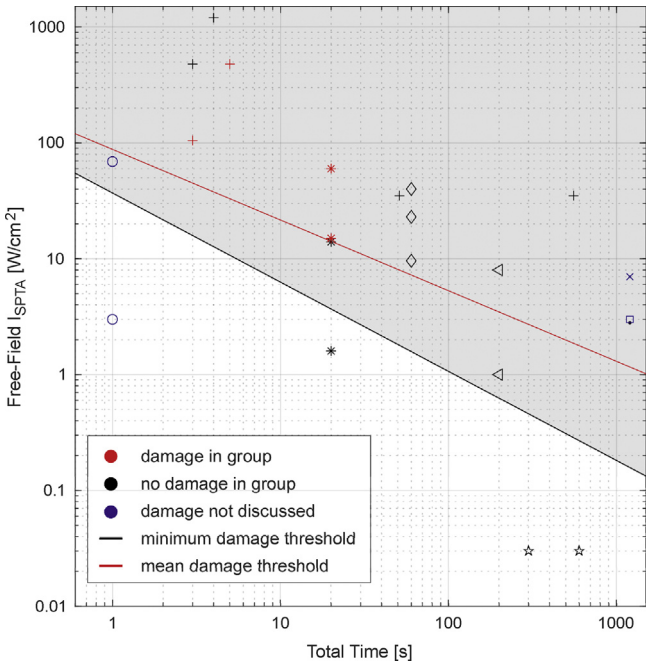

Figure 5. Spinal cord neuromodulation studies plotted by spatial peak time-averaged intensity (I_{SPTA}) and total treatment time. *Red* denotes damage, *black* denotes no damage, and *blue* denotes studies in which damage was not discussed. o, Takagi et al. 1960 [138]; +, Ballantine et al. 1960 [3]; *, Liao et al. 2021 [19]; •, Liao et al. 2021 [69]; ×, Liao et al. 2022 [139]; □, Wang et al. 2022 [140]; ◁, Kim et al. 2022 [20]; ☆, Tseha et al. 2023 [21]; ◇, Song et al. 2023 [22]. The previously fit minimum (*black line*) and mean (*red line*) damage thresholds (from Fig. 3) are plotted for reference.

The sample sizes of the neuromodulatory studies are also smaller than those of the spinal cord damage studies (often by an order of magnitude), so exposures with low damage probability may not have been sufficiently sampled for damage to be detected.

The relative importance of thermal versus mechanical mechanisms in ultrasonic spinal cord neuromodulation remains an open question in the field. The time dependence in Figure 5 suggests that heating plays a role in spinal cord neuromodulation, and the identified spinal cord neuromodulation studies present limited evidence that agrees. Three of the neuromodulatory studies measured temperature throughout the sonications [20–22], recording temperature rises of 0.5°C and higher. Although these temperature rises are several times smaller than those measured in the spinal cord damage studies, they do not exclude heating as a driver of neuromodulatory activity, as the threshold for heat-based neuromodulatory effects in the spinal cord has been cited as 0.5°C [70], and temperature changes in the spinal cord are known to drive change in other neural circuits [71–74]. Whole-body heating to a mean core temperature of 38.7°C has been tested in humans [75], where it was also found that the raised core temperature reduced modulation in the human spinal cord. Heating may also modulate mechanical force-based neuromodulatory effects of ultrasound [76,77], as some of the responsible mechanosensitive ion channels are also modulated by temperature [78,79]. A recent study compared the neuromodulatory effect of direct heat with that of focused ultrasound, finding that both suppressed H-reflex amplitude but only ultrasound reduced the H-reflex latency [22]. It may not be necessary to design experiments or therapies that avoid any thermal effects; if the conversion of ultrasound energy to heat energy at a specific target can achieve an intended neuromodulatory effect at the target while keeping the temperature elevation below a safe threshold, then it should remain a viable experiment or therapy.

The second concern may be more difficult to address, but it is promising that several of the studies do not exceed the minimum damage threshold, and one of the studies were conducted with an I_{SPTA}

Table 3
Pre-clinical focused ultrasound spinal cord neuromodulation studies

Reference	Subject	n	Frequency	Sonication mode	Time (s)	I_{SPPA}	I_{SPTA}	Damage	Neuromodulation
Takagi et al. 1960 [138]	Toad (cord)	1	1	Continuous	1	3–69	3–69	?	Discharges
Ballantine et al. 1960 [3]	Cat (lam.)	11	2.7	0.3 s pulse, 0.33 Hz	51–555	350	35	No	Reflex ↑ or ↓
	Cat (lam.)	5	2.7	0.3 s pulse, 1 Hz	3	350	105	No	Reflex ↑
	Cat (lam.)	1	2.7	0.3 s pulse, 1 Hz	4	4000	1200	Yes	Reflex ↑
	Cat (lam.)	9	2.7	0.3 s pulse, 1 Hz	<3	1600	480	No	Reflex ↑
	Cat (lam.)	14	2.7	0.3 s pulse, 1 Hz	>5	1600	480	Yes	Reflex ↑
Liao et al. 2021 [19]	Rat	24	4	200 μs pulse, 1 kHz	20	8–75	1.6–15	No	Recruitment ↑
	Rat	24	4	200 μs pulse, 1 kHz	20	75–300	15–60	Yes	Recruitment ↑
Liao et al. 2021 [69]	Rat	40	4	250 μs pulse, 0.8 kHz	1200	14	2.8	No	Injury recovery
Liao et al. 2022 [139]	Rat (lam.)	30	4	625 μs pulse, 0.8 kHz	1200	14	7	?	↓ Spasticity
Wang et al. 2022 [140]	Rat (lam.)	18	1	250 μs pulse, 0.8 kHz	1200	15	3	?	↓ Spasticity
Kim et al. 2022 [20]	Mouse	50	3	0.2 s train,[a] 0.5 Hz	200	21–161	1–8	No	↓ Descending
	Mouse	50	3	0.2 s train,[a] 0.5 Hz	200	65–161	3–8	No	↑ Descending
Tseha et al. 2023 [21]	Rat (lam.)	10	0.5	500 μs pulse, 1 kHz	300–600	0.06	0.03	No	↓ MEP
Ahmed 2023	Rat (lam.)	30	1	200 μs pulse, 1 kHz	600	0.07	0.014	?	↑ grasp strength
Song et al. 2023	Rat	35	1.1	200 μs pulse, 2 kHz	60	24-99	9.6-40	No	Reflex amp. ↓
	Rat	35	1.1	4 ms pulse, 100 kHz	60	73	29	No	Reflex amp. ↑

Reported parameters include the sample size (n), frequency (MHz), I_{SPPA} and I_{SPTA} (both in W/cm^2), details regarding damage and neuromodulatory effect (MEP). This table does not include Shealy 1962 [4] (unknown intensities). The Liao 2021b, Liao 2022, and Wang 2022 experiments repeated the 1200 s exposures daily for 4 wk.
I_{SPPA}, spatial peak pulse averaged intensity; I_{SPTA}, spatial peak time averaged intensity; lam., laminectomy; MEP, motor evoked potential.
[a] Kim 2022 pulse trains contained 500 μs pulses (1 kHz pulse repetition frequency).

approximately an order of magnitude lower than the threshold [21]. Of the studies that exceeded the threshold, only one was performed in mice [20]; the remainder were performed in rats or cats, which may be more resistant to thermal damage because of their larger masses and greater ability to remove heat via perfusion. The intact spines of the rats used in several of the studies will also have reduced the intensities relative to the free-field values [19,22,69]. The mouse neuromodulation study performed by Kim et al. [20] found no damage, yet had I_{SPTA} versus exposure time parameters similar to those of the Stolzenberg et al. [40] ablation study that found damage at 100–120 s. However, the transducer used in Stolzenberg et al. [40] produced a broad 3 cm diameter focal zone, while the source used in Kim et al. [20] produced a 3 mm diameter focus. The Stolzenberg source would therefore have delivered approximately 100 times more total ultrasonic energy to the animal, so it is perhaps unsurprising that damage occurred at the minimum threshold line in the Stolzenberg et al. study [40], while damage was not observed in the Kim et al. study [20]. The damage discrepancy between these two studies demonstrates that although the minimum thresholds may be a useful tool with which to judge the possibility of damage, a careful consideration of all ultrasonic parameters, perhaps through combined acoustic and thermal simulation, is necessary to fully understand the damaging potential of an ultrasonic treatment.

Blood–spinal cord barrier opening

Several of the early spinal cord studies noted haemorrhage in damaged spinal cords in the 1950s to 1970s [38,42,43], indicating that disruption of the normal spinal cord vasculature was possible through the application of sufficiently intense ultrasound. However, it was not until after 2001 when a study determined that the blood–brain barrier could be opened with ultrasound and microbubbles in a reversible and repeatable manner [80] that interest in performing BSCBo for therapeutic agent delivery was piqued, and the first BSCBo study was published in 2005 [10].

Figure 6 depicts all of the identified BSCBo studies (with independent and identifiable parameters) with the "potential damage" thresholds plotted for reference. The BSCBo studies reveal that the minimum and mean damage thresholds have no predictive ability for vascular or spinal cord damage. This is because the BSCBo studies incorporate pre-formed microbubbles injected into the vasculature, which can generate mechanical (cavitation) effects at much lower pressures than are needed to generate de novo cavitation. The thresholds for damage may instead be linked to a combination of the peak negative pressure or the mechanical index [81], the microbubble dose [82] or the microbubble gas volume [83], and the interactions between microbubbles and the ultrasound parameters (*e.g.,* pulse duration and pulse repetition frequency will have an effect on bubble depletion within the focal region) [84]. The number of linked parameters for damage in the presence of microbubbles is impractical to visualize, particularly with the addition of feedback controllers that change pressures based on recordings of real-time microbubble emissions [85], and the addition of pulse trains containing short (*i.e.,* a few cycles) pulses and that incorporate phase keying (which may interact with microbubbles in a different way than pulses that do not use phase keying) [86,88]. For example, Figure 7 plots damage against two parameters known to influence vascular disruption (mechanical index [81] and microbubble dose [82]) and illustrates that these two parameters alone also cannot explain BSCBo damage thresholds. A comprehensive statistical analysis of all of the tested parameters to identify their effects on damage probability could potentially be performed, but the number of BSCBo studies and the range of parameters tested are likely still too limited to obtain meaningful trends. An abbreviated set of the parameters implemented in the studies plotted in Figures 6 and 7 and discussed in Appendix S3 (online only) are summarized in Table 4. Further details from each study are compiled in the Supplementary Material (online only).

Each of the studies in Table 4 successfully performed BSCBo, measured using the extravasation of a contrast agent [18,25,87–93] or the quantification of the increased delivery of a potential therapeutic agent in the target tissues [10–16,18,94]. While achieving BSCBo was generally successful (with the exception of the porcine intact spine model, which required much higher pressures and resulted in variable and spinal level = dependent BSCBo), many of the studies observed minor to major damage in the target tissues upon histological examination.

Trends in ultrasound-induced damage are not explained by the minimum or mean damage thresholds (Fig. 6) and only partially by mechanical index and microbubble dose (Fig. 7). Safety simulations for BSCBo may be used to estimate in situ pressure distributions, standing wave formation and tissue heating, particularly given the additional ultrasonic attenuation and heating that results from systemically administered microbubbles. However, the best way to avoid ultrasound-induced

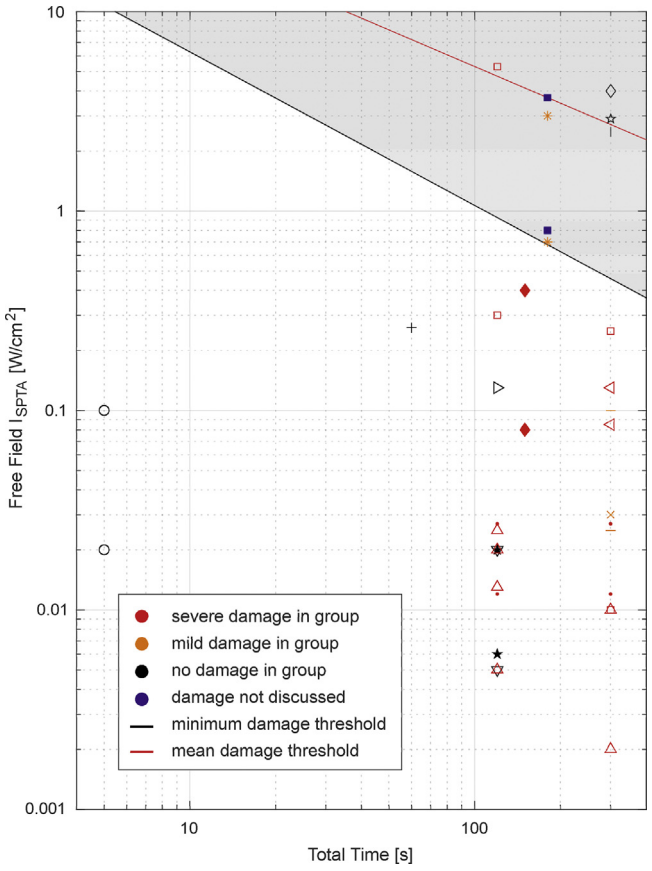

Figure 6. Blood–spinal cord barrier opening studies plotted by spatial peak time-averaged intensity (I_{SPTA}) and total treatment time. *Red* denotes ultrasound-induced damage, *yellow* denotes damage caused by other means, *black* denotes no damage, *blue* denotes studies in which damage was not discussed. o, Shimamura et al. 2005 [10]; +, Takahashi et al. 2007 [11]; −, Wachsmuth et al. 2009 [88]; ◁, Oakden et al. 2014 [141]; ×, Weber-Adrian et al. 2015 [13]; |, Song et al. 2017 [14]; *, Payne et al. 2017 [91]; ◇, Song et al. 2018 [15]; ▽, O'Reilly et al. 2018 [16]; ◆, Montero et al. 2019 [25]; •, → Fletcher et al. 2019 [89]; ▷, → Shah 2020 [17]; □, Fletcher et al. 2020 [90]; ★, Smith et al. 2021 [18]; ■, Cross et al. 2021 [92]; △, Fletcher et al. 2021 [87]; ☆, Bhimreddy et al. 2023 [93]. The previously fit minimum (*black line*) and mean (*red line*) damage thresholds (from Fig. 3) are plotted for reference.

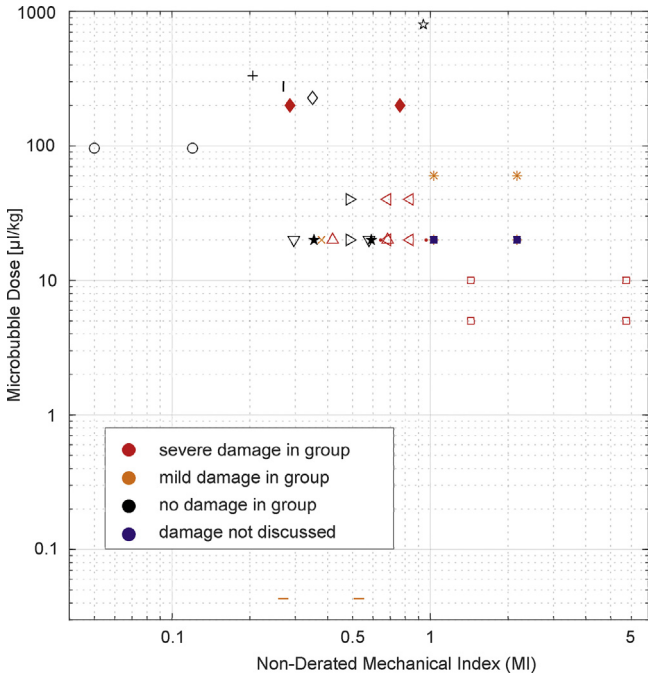

Figure 7. Blood–spinal cord barrier opening studies plotted against the non-derated mechanical index (MI) and the microbubble dose. *Red* denotes ultrasound-induced damage, *yellow* denotes damage caused by other means or minor damage, *black* denotes no damage, *blue* denotes studies in which damage was not discussed. O, Shimamura et al. 2005 [10]; +, Takahashi et al. 2007 [11]; −, Wachsmuth et al. 2009 [88]; ◁, Oakden et al. 2014 [141], ×, Weber-Adrian et al. 2015 [13]; |, Song et al. 2017 [14]; *, Payne et al. 2017 [91]; ◇, Song et al. 2018 [15]; ▽, O'Reilly et al. 2018 [16]; ◆, Montero et al. 2019 [25]; •, Fletcher et al. 2019 [89]; ▷, Shah 2020 [17]; □, Fletcher et al. 2020 [90]; ★, Smith et al. 2021 [18]; ■, Cross et al. 2021 [92]; △, Fletcher et al. 2021 [87]; ☆, Bhimreddy et al. 2023 [93].

damage may be to use a feedback control algorithm to limit the exposures based on microbubble emission spectra [16,18,85], although this algorithm may require modification for safe usage in large animal models [90] or eventually in humans. Intraprocedural cavitation localization may further improve the safety of BSCBo by giving the operators useful spatial information on the bubble activity [95].

Despite the evidence of mild to major damage in several of the identified BSCBo studies, only one study reported the ultrasound-induced paralysis or paraplegia that was discussed in the Ablation and Damage section of this review, and this paralysis may be linked to cold microbubble injection [13]. Perhaps modern histological methods have improved to the extent that haemorrhage or other damage can be discovered before the point of paralysis, which would counter the historical articles that found that tissue exposed to an ultrasound exposure below the minimum damage threshold was indistinguishable from normal tissue [34]. However, many of the studies discussed in this section were acute studies and did not specifically investigate paralysis/paraplegia. Further investigations into the safety of BSCBo with feedback control are warranted, and longitudinal studies performed in large animals would be particularly useful.

This literature review does not include the many (hundreds of) ultrasound and microbubble blood–brain barrier opening studies; a meta-analysis of blood–brain barrier opening studies may unveil stronger trends in damage versus the many parameters used during these treatments [49,84].

Future directions

A substantial amount of work has been performed in pre-clinical studies investigating applications of focused ultrasound to the spinal cord. When amassed, these studies illustrate useful trends in intensity versus exposure time for observed damage and demonstrate the need for active monitoring and control of ultrasound exposures when pre-formed microbubbles have been systemically injected. Further trends (*e.g.,* sonication parameters vs. neuromodulatory effect size) may be elucidated from existing and future pre-clinical studies. The utility of existing and future studies in developing these trends depends on the clear and accurate communication of the implemented ultrasound exposure conditions. Guidelines for reporting ultrasound exposure parameters have been published [96,97] that, if followed, will ensure that future work contains the necessary details for cross-study comparisons and reviews. Standardized reporting guidelines for focused ultrasonic neuromodulation in humans are also being developed by the International Transcranial Ultrasonic Stimulation Safety and Standards (ITRUSST) group. Future studies may also consider reporting where their implemented ultrasound exposure parameters lie relative to Eqns. (3) and (4) and discuss differences between their implemented parameters and those implemented in the studies defining the thresholds.

Pre-clinical studies alone have not yet answered all the safety questions that need to be addressed, so it is worthwhile considering what is required to translate spinal cord neuromodulation and blood–spinal cord barrier opening to the clinical scale. Safety remains one of the main

Table 4
Pre-clinical focused ultrasound blood–spinal cord barrier opening studies

Reference	Subject	n	Bubbles	Frequency (MHz)	Sonication mode	Time (s)	Peak pressure (MPa)	I_{SPTA} (W/cm^2)	Damage
Shimamura et al. 2005 [10]	Rat	40	25 μL Opt.	1	20% duty cycle	5	0.05–0.12	0.02–0.1	No
Takahashi et al. 2007 [11]	Mouse	60	<10 μL Opt.	0.95	20% duty cycle	60	0.2	0.26	No
Wachsmuth et al. 2009 [88]	Rat	31	0.043 μL/kg Def.	1.08	20 ms pulse, 1 Hz	300	0.28–0.55	0.025–0.1	In 16%
Ando et al. 2011 [94]	Rat	40	N/A	N/A	Photomechanical	?	45/5	?	N/A
	Rat	20	N/A	N/A	Photomechanical	?	135/3	?	N/A
Ando et al. 2012 [12]	Rat	40	N/A	N/A	Photomechanical	?	50/8	?	N/A
Oakden et al. 2014 [142]	Rat	19	20–40 μL/kg Def.	1.114	10 ms pulse, 0.5 Hz	300	0.72–0.88	0.085–0.13	Yes
Oakden et al. 2015 [142]	Rat	16	20–40 μL/kg Def.	1.114	10 ms pulse, 0.5 Hz	300	0.88	0.13	Yes
Weber-Adrian et al. 2012 [13]	Rat	12	20 μL/kg Def.	1.114	10 ms pulse, 0.5 Hz	300	0.4	0.03	In 8%
Song et al. 2017 [13]	Rat	158	50 μg NB	1?	Continuous	300	0.27	2.5	No
Payne et al. 2017 [91]	Rat	14	20–60 μL/kg Opt.	0.94	20 ms pulse, 1 Hz	180	1.0–2.1	0.7–3	20%
Song et al. 2018 [14]	Rat	92	50 μg NB	1?	Continuous	300	0.35	4	No
O'Reilly et al. 2018 [15]	Rat	18	20 μL/kg Def.	0.552	10 ms pulse, 1 Hz	120	0.22–0.43	0.005–0.02	No
Montero et al. 2019 [24]	Rabbit	15	200 μL/kg Sono.	1.1	25 ms pulse, 1 Hz	150	0.3–0.8	0.08–0.4	Yes
Fletcher et al. 2019 [89]	Rat	7	20 μL/kg Def.	0.514	10 ms train,[a] 1 Hz	120	0.46–0.69	0.01–0.03	Yes
Shah 2020 [16]	Mouse	51	20–40 μL/kg Def.	1.68	10 ms pulse, 1 Hz	120	0.62–0.64	0.13	No
Fletcher et al. 2020 [90]	Pig	4	5–10 μL/kg Def.	0.486	10 ms pulse, 1 Hz	120	1.0–4.0	0.3–5.3	Yes
	Pig	4	5–10 μL/kg Def.	0.486	10 ms train,[a] 1 Hz	300	1.0–2.1	0.01–0.25	Yes
Smith et al. 2021 [17]	Rat	13	20 μL/kg Def.	0.58	20 ms pulse, 1 Hz	120	0.36	0.006–0.02	No
Cross et al. 2021 [92]	Rat	24	20 μL/kg Opt.	0.94	25 ms pulse, 1 Hz	180	1.0–2.1	0.8–3.7	?
Fletcher 2021	Rat	12	20 μL/kg Def.	0.514	5 ms train,[a] 1 Hz	120	0.3–0.49	0.005–0.025	Yes
	Rat	4	20 μL/kg Def.	0.514	2 ms train,[a] 1 Hz	300	0.42	0.002	Yes
	Rat	4	20 μL/kg Def.	0.514	10 ms train,[a] 1 Hz	300	0.42	0.01	Yes
Bhimreddy 2023	Rat	5	0.8 mL/kg Lum	0.25	0.4 s pulse, 1 Hz	300	0.47	2.9	No

I_{SPTA}, spatial-peak time-averaged intensity; Def, Definity; Lum, Lumason; Opt, Optison; Sono, SonoVue.
[a] Denotes pulse trains containing short 2 to 5 cycle pulses with phase keying repeated at 20 to 40 KHz [87,89,90].

translational challenges; it has been discussed at length in the context of pre-clinical models, but additional challenges may arise in humans. One challenge is obtaining a coherent focus within the vertebral canal; many studies have used laminectomies to enable the generation of a coherent focus at the intended target, but this alone does not guarantee the in situ field will resemble the free-field pressure distribution. Laminectomies are highly invasive procedures and, unless pre-existing from another surgery, are unlikely to be accepted as part of a treatment plan. This means that focusing ultrasound through the human spine to the spinal cord will be necessary. Another translational challenge may be target selection. Some targets may be focal and near the centre of the spinal cord; other targets may be diffuse and dispersed throughout the spinal canal. Different targets are likely to require different approaches to obtaining the desired bio-effects while avoiding unintended bio-effects elsewhere. These translational challenges are discussed in the following subsections.

Safety

Pre-clinical findings have demonstrated a clear relationship between damage, I_{SPTA} and total treatment time, the importance of performing feedback control in studies that rely on microbubble-mediated bio-effects and the importance of performing simulations to estimate the in situ pressure distributions and heating patterns. However, additional safety concerns will need to be addressed before the translation of focused ultrasound spinal cord therapies to humans.

The spine is a complex, irregular bony structure, with several characteristics of importance for focused ultrasound spinal cord studies. One characteristic is the posterior intervertebral gaps between vertebrae. These gaps provide acoustic windows through the spine to certain spinal cord targets. However, a potential drawback of these acoustic windows may be mode conversion and shear wave transmission into the vertebrae at non-normal incident angles [23] and subsequent bone heating from shear wave attenuation. A spinal characteristic that has been briefly discussed is the cylindrical geometry of the spinal canal, which is susceptible to standing wave formation at certain vertebral levels [86]. It is essential that this field avoids the situation that occurred in the TRUMBI study, where a set of planar 300 kHz transducers and a tissue plasminogen activator were used to treat brain clots. The study had to be ended early because five patients developed cerebral hemorrhages and one patient died. A later study suggested that standing waves and excessive pressures caused the cerebral hemorrhages [98]. An approach using phased-keyed short pulses was developed to minimize standing wave formation and uncontrolled pressure fields in the vertebral canal, outperforming chirp/swept frequency pulses or longer unmodulated pulses [86,89]. Relatively few studies have investigated the safety and bubble response to these phase-keyed short pulses (in comparison to the longer pulses used for blood–brain barrier opening), and future studies should investigate their safety in greater detail. Another characteristic of human vertebrae is the shape of their laminae when viewed from a vertical perspective; they are parabolic, making them ideal reflectors and liable to generate paravertebral tissue heating [24,95]. Finally, the vertebral canal is narrow, with little distance separating the spinal cord from the vertebrae. Ultrasound energy absorbed by the vertebrae as heat may dissipate into the spinal cord. This was reported to be the cause of some spinal cord damage in Borrelli et al. [34], where damage was limited to the ventral portion of the spinal cord, nearest to the vertebral bodies.

Focusing ultrasound to the spinal cord remains a challenge. It may not be possible to reach certain targets through the posterior intervertebral gaps, particularly in the flexion-limited thoracic spine [99]. The esophagus occludes anterior paths to the spinal cord at the cervical level; the rib cage and lungs occlude anterior and lateral paths in the thoracic spine; and potentially gas-filled internal organs occlude anterior acoustic paths to the lumbar spinal cord. It is possible to generate a trans-spine focus with an extracorporeal single-element focused transducer [24,86,100] or a dual-aperture approach [87,89,91], focused through the posterior elements of the spine. However, the focus in some transducer positions will inevitably be aberrated, shifted by several millimetres, or split into several subfoci by spine-induced wavefront aberrations [24], much like a focus aberrated by trans-skull propagation. In these cases, the intended bio-effects may not occur in the desired location or at all. Unless a target happens to be one that permits the use of a single-element

transducer with minimal aberration, then some form of aberration correction method will be needed to obtain a focus at the intended target location [99]. Several aberration correction methods exist for transcranial applications, including phased arrays [6,101] or 3-D-printed acoustic lenses [102,103]. Equivalent spine-specific arrays intended for focusing ultrasound to the vertebral canal have been optimized in simulation [99] and partially tested in a preliminary ex vivo experiment [104]. Spine-specific arrays for intervertebral disc therapies have also been discussed and simulated [105,106], but none have reached a level of clinical adoption. Both development and characterisation of arrays capable of focusing ultrasound through the vertebral canal and the development of accurate image registration and array-patient registration methods are necessary for the advancement of the focused ultrasound spinal cord field.

Methods for obtaining trans-spine aberration corrections still require further development. An implanted/virtual source method has been simulated for focusing sound to targets within the vertebral canal, generating phase corrections [99], or to the nearby intervertebral discs, to perform time reversal-based beamforming [105]. However, implanting an ideal source in the spinal cord is unlikely to be feasible in practice (although interstitial sources have been investigated for tumour ablation in the vertebral canal [107]). In microbubble-based procedures, microbubble emissions may potentially be used to improve targeting in a similar "guide star" like manner to atmospheric wavefront distortions [108]. This method has been tested with ex vivo skulls [109] and for essential tremor thalamotomies with promising results [110], but still relies on initial simulation-based calculations. Simulations alone can generate phase corrections or act as a beamforming algorithm; this has been tested at length for trans-skull ultrasonic focusing with large multi-element arrays [111,112]. Studies have investigated simulation accuracy in predicting trans-spine ultrasound focusing [24] and used this modelling to optimise a method to convert CT-derived vertebral lamina densities to sound speed, a crucial component to performing CT-based simulations for aberration correction. However, these modelling studies have been limited to many fewer simulation methods than trans-skull work [113] and to just one single *ex vivo* spine [23,24,95,104]. It will be important to replicate these studies with new samples and different simulation methods in order to build consensus on the translation of trans-skull ultrasonic methods to trans-spine focused ultrasound applications [113].

Once sound is successfully delivered to the spinal cord, then any intended or unintended bio-effects should be monitored to ensure the safety of the procedure. This will be particularly important if the parameters are close to the minimum damage threshold or if microbubbles are systemically injected. Heating may be non-invasively monitored with MR thermometry; a proof-of-concept study suggests that temperature measurement in the nearby dorsal root ganglions is possible [114]. However, MR temperature measurement in cortical bone is not possible because of the lack of mobile protons, and MR thermometry might not be able to measure hot spot formation on the vertebral surfaces. Ensuring that temperature rises do not exceed a safe threshold in cortical bone may be the domain of validated acoustic and thermal simulation. The spatial mechanical effects of focused ultrasound in the presence of microbubbles may be monitored with acoustic receivers and passive acoustic mapping [95], although this method has yet to be demonstrated experimentally. Therapies that use parameters well below the minimum damage threshold and do not involve microbubbles may not require rigorous thermal and mechanical bio-effect monitoring methods, but the outcome (*e.g.,* neuromodulatory) effects should still be monitored by other available means.

Targets

A focused ultrasound treatment must by definition have a target. The target will be based on a disease or medical condition and how it presents in a specific patient, as well as the intended bio-effects of the focused ultrasound treatment. For example, spinal cord injuries can occur at any level, although they tend to be most common at the cervical level, then thoracic, then lumbar levels [115]. A focused ultrasound therapy intended to treat spinal cord injury, either via improved therapeutic agent delivery to the injured tissue, stem cell stimulation [116] or "offline" neuromodulatory or neuroplastic effects sustained post-treatment [15,66–68] may require a different ultrasonic strategy based on the target. A diffuse disease (*e.g.,* spinal muscular atrophy, where treatment [117] efficiency may be improved with BSCBo [13]) would still require point-by-point or region-by-region targeting to expose the whole spinal cord.

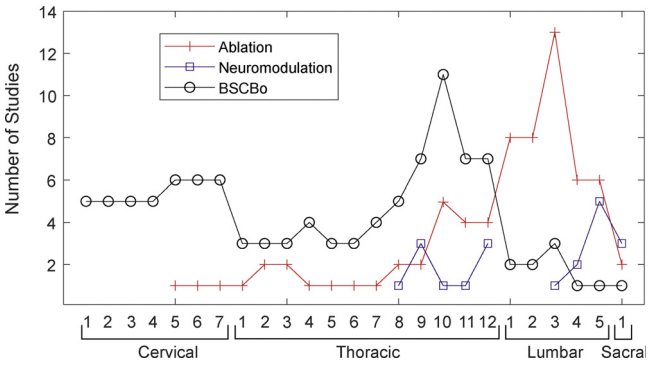

Figure 8. Spinal cord targets. Damage, neuromodulation and blood–spinal cord barrier opening (BSCBo) studies have investigated targets spanning the spine.

The spinal cord targets used in all studies discussed here are listed in the Supplementary Material (online only) and plotted in Figure 8. There are some trends in target level; most of the spinal cord damage studies describe targeting in the low thoracic to lumbar region, most likely to enable the identification of hindlimb paralysis/paraplegia. Neuromodulation studies follow a similar trend, perhaps again to isolate the bio-effects to the lower limbs. The BSCBo studies used targets that span most of the spinal cord, with slightly fewer in the lumbar spine. The referenced studies investigate a wide range of targets. Studies that focused ultrasound to an entire region (*e.g.,* dorsal, cervical, thoracic, thoracolumbar or lumbar) are represented at each level, while studies that targeted a single level are only represented at that level. Spine morphology and number of vertebrae differ across the tested animal models, so the reference levels in Figure 8 are an estimated representation of the equivalent level in a human spine. When future studies are performed, this may be a useful starting point for choosing a target level in an animal model.

Any treatment intending to affect a specific spinal cord nerve, damaged region of the spinal cord or focal tumour will be targeted based on the afflicted region. It is unlikely that (at the writing of this review) a study will have been performed with the specific parameters for that target. The safety of the treatment should therefore be demonstrated before the treatment. Simulation is one potential method to demonstrate safety across a large set of parameters; given patient-specific imaging and proper patient–image–source registration, it may be possible to accurately calculate the treatment mechanical forces and heat deposition and ensure that they remain within safe limits. Similarly, given a large enough image data set, a simulation study could be performed before an in vivo study to establish the safety of a specific set of ultrasonic parameters for a given target. When safe limits for heat deposition and mechanical index are established and accepted for BSCBo and neuromodulation, and simulation accuracy is established and accepted for predicting these in situ values, simulation-based safety studies could accelerate the field of focused ultrasound spinal cord therapies.

This review has focused on spinal cord targets throughout. However, other targets surrounding the spinal cord have been investigated at various levels. For example, there is substantial pre-clinical research investigating the delivery of ultrasound to intervertebral disks [105,106,118–122], the ablation of facet joints [123–126], and the ablation or

neurostimulation of lumbar nerves or dorsal root ganglions [127–130]. Ultrasound has also been used to deliver energy to drive piezoelectric stimulators in rat spinal cords [131]. These studies employ strategies that may prove useful for spinal cord-targeting therapies. For example, Zhang et al. [125] used a thermochromic spine phantom based on a human CT scan to investigate heating in a potential facet joint ablation treatment. This phantom-based approach could be used to validate safety simulations and independently demonstrate the safety of a potential focused ultrasound spinal cord therapy, particularly if extended to a range of phantoms that represent a normal range in human anatomical variation and bone density.

The physiotherapeutic use of ultrasound for low back pain was not discussed in this review as such a review has been published recently [132], and opinions are mixed regarding the utility of this treatment. There have been instances where the application of physiotherapeutic ultrasound to the spine had deleterious side effects [133]. For continuous or pulsed intensities of 0.1–3 W/cm^2, there appears to be little to no benefit of using ultrasound to treat chronic back pain, and the targeting in these physiotherapeutic studies is generally vague [132]. For example, the targeting is described in one article as follows: slow circular movements were applied using the transducer head over the paravertebral region, aiming for a local exposure time of one minute [134]; thermal dose and in situ pressures between patients is likely to be highly operator-dependent and difficult to reproduce.

Studies have also investigated ultrasonic methods for performing ablation of tumours in the spine and near the spinal cord using a percutaneous/interstitial source [107,135]. Strategies developed for source guidance and control and monitoring in these works may be useful for focused ultrasound spinal cord therapies, despite differences in the percutaneous/interstitial approach versus a non-invasive approach.

The spine and spinal cord are critical to motor control, sensation, reflex arcs and providing the structural support for most of the human body. With its many roles and many possible diseases and disorders, there are many possible targets for focused ultrasound therapies. It will be interesting to see what targets are identified and the paths taken to demonstrate the safety and efficacy of potential therapies. It is hoped that this review provides a useful foundation for the safe development of spinal cord therapies and relevant safety guidelines.

Conclusion

There is a renewed interest in focusing ultrasound on the spinal cord, particularly for blood–spinal cord barrier opening for improving therapeutic agent delivery to the spinal cord and for the neuromodulation of ascending or descending tracts of the spinal cord. However, it remains crucial that historical papers from the early days of focused ultrasound be considered when designing new studies and potential therapies. These historical papers investigated the damage to the spinal cord in several pre-clinical models and in large numbers to understand trends in damage versus exposure duration and intensity. This review collates the data across animal models and reveals a clear relationship between time-averaged spatial peak intensity and exposure duration and damage, independent of animal model and various different tested environmental conditions. Equations were fit to the pre-clinical data to create minimum and mean thresholds for the reported damage across studies, then these thresholds were compared with the intensities and exposure durations used in recent neuromodulation studies. Although some of the neuromodulation studies were below the minimum threshold, the majority of the studies were near or above this threshold. Neuromodulatory pulse sequences that rely on a thermal effect that approach this threshold must be carefully controlled to avoid damage and possible paralysis or paraplegia.

When applied to the blood–spinal cord barrier opening studies that employed injected contrast agents (microbubbles or nanobubbles) to enhance the redistribution of ultrasonic energy to the vasculature, the intensity–exposure duration threshold had little to no predictive value. Most blood–spinal cord barrier opening studies observed slight to severe damage, except for studies that employed an active feedback control method to limit pressures based on the measured bubble oscillation behaviour. Although successful in small animals, this feedback control method did not prevent damage in a porcine model, suggesting that the controller may need further optimisation for spinal cord-focused ultrasound therapies. The development of blood–spinal cord barrier opening and ultrasonic spinal cord neuromodulation perhaps reflects the recent successes in the development of focused ultrasound brain applications, and recent work has begun on the translation of these technologies from brain to spinal cord through the complex spine. However, there remains a great deal of work, particularly with respect to developing and accepting safety standards for these potential treatments. May the rapid growth in blood–spinal cord barrier opening studies and focused ultrasound spinal cord neuromodulation studies continue, safely.

Data availability statement

The data collected during this review are available as supplementary material.

Conflict of interest

The authors declare no competing interests.

Acknowledgments

This work was supported in part by a UKRI Future Leaders Fellowship (Grant MR/T019166/1) and in part by the Wellcome/EPSRC Centre for Interventional and Surgical Sciences (WEISS) (No. 203145Z/16/Z). For the purpose of open access, the author has applied a CC BY public copyright licence to any Author Accepted Manuscript version arising from this submission. The authors thank Professor Sven Bestmann and Dr. Carys Evans for useful discussions on this work.

Supplementary materials

Supplementary material associated with this article can be found in the online version at doi:10.1016/j.ultrasmedbio.2023.11.007.

References

[1] Fry WJ, Wulff VJ, Tucker D, Fry FJ. Physical factors involved in ultrasonically induced changes in living systems: I. Identification of non-temperature effects. J Acoust Soc Am 1950;22:867–76.
[2] Fry WJ, Tucker D, Fry FJ, Wulff VJ. Physical factors involved in ultrasonically induced changes in living systems: II. Amplitude duration relations and the effect of hydrostatic pressure for nerve tissue. J Acoust Soc Am 1951;23:364–8.
[3] Ballantine HT, Bell E, Manlapaz J. Progress and problems in the neurological applications of focused ultrasound. J Neurosurg 1960;17:858–76.
[4] Shealy CN, Henneman E. Reversible effects of ultrasound on spinal reflexes. Arch Neurol 1962;6:374–86.
[5] Bartanusz V, Jezova D, Alajajian B, Digicaylioglu M. The blood–spinal cord barrier: morphology and clinical implications. Ann Neurol 2011;70:194–206.
[6] Lipsman N, Michael L, Schwartz ML, Huang Y, Lee L, Sankar T, et al. MR-Guided focused ultrasound thalamotomy for essential tremor: a proof-of-concept study. Lancet Neurol 2013;12:462–8.
[7] Lipsman N, Meng Y, Bethune AJ, Huang Y, Lam B, Masellis M, et al. Blood–brain barrier opening in Alzheimers disease using MR-guided focused ultrasound. Nat Commun 2018;9:1–8.
[8] Mainprize T, Lipsman N, Huang Y, Meng Y, Allison Bethune A, Ironside S, et al. Blood–brain barrier opening in primary brain tumors with non-invasive MR-guided focused ultrasound: a clinical safety and feasibility study. Sci Rep 2019;9:1–7.
[9] Abrahao A, Meng Y, Llinas M, Huang Y, Hamani C, Mainprize T, et al. First-in-human trial of blood–brain barrier opening in amyotrophic lateral sclerosis using MR-guided focused ultrasound. Nat Commun 2019;10:1–9.
[10] Shimamura M, Sato N, Taniyama Y, Kurinami H, Tanaka H, Takami Y, et al. Gene transfer into adult rat spinal cord using naked plasmid DNA and ultrasound microbubbles. J Gene Med 2005;7:1468–74.
[11] Takahashi M, Kido K, Aoi A, Furukawa H, Ono M, Kodama T. Spinal gene transfer using ultrasound and microbubbles. J Control Release 2007;117:267–72.
[12] Ando T, Sato S, Toyooka T, Kobayashi H, Nawashiro H, Ashida H, et al. Photomechanical wave-driven delivery of siRNAs targeting intermediate filament proteins promotes functional recovery after spinal cord injury in rats. PLoS One 2012;7:e51744.

[13] Weber-Adrian D, Thevenot E, O'Reilly MA, Oakden W, Akens MK, Ellens N, et al. Gene delivery to the spinal cord using MRI guided focused ultrasound. Gene Ther 2015;22:568–77.
[14] Song Z, Wang Z, Shen J, Xu S, Hu Z. Nerve growth factor delivery by ultrasound-mediated nanobubble destruction as a treatment for acute spinal cord injury in rats. Int J Nanomed 2017;12:1717.
[15] Song Z, Ye Y, Zhang Z, Shen J, Hu Z, Wang Z, et al. Noninvasive, targeted gene therapy for acute spinal cord injury using LIFU mediated BDNF-loaded cationic nanobubble destruction. Biochem Biophys Res Commun 2018;496:911–20.
[16] O'Reilly MA, Chinnery T, Yee ML, Wu SK, Hynynen K, Kerbel RS, et al. Preliminary investigation of focused ultrasound-facilitated drug delivery for the treatment of leptomeningeal metastases. Sci Rep 2018;8:1–8.
[17] Shah KA. MSc Thesis. Toronto, Canada: University of Toronto; 2020.
[18] Smith P, Ogrodnik N, Satkunarajah J, O'Reilly MA. Characterization of ultrasound-mediated delivery of trastuzumab to normal and pathologic spinal cord tissue. Sci Rep 2021;11:1–12.
[19] Liao YH, Chen MX, Chen SC, Luo KX, Wang B, Liu Y, et al. Effects of noninvasive low-intensity focus ultrasound neuromodulation on spinal cord neurocircuits in vivo. Evid Based Complement Alternat Med 2021;2021:8534466.
[20] Kim E, Kum J, Kim H. Trans-spinal focused ultrasound stimulation selectively modulates descending motor pathway. IEEE Trans Neural Syst Rehabil Eng 2022;30:314–20.
[21] Tseha Y, Zeng Y, Weber-Levine C, Awosika T, Kerensky M, Hersh AM, et al. Low-intensity pulsed ultrasound neuromodulation of a rodent's spinal cord suppresses motor evoked potentials. IEEE Trans Biomed Eng 2023;70:1992–2001.
[22] Song W, Jayaprakash N, Saleknezhad N, Puleo C, Al-Abed Y, Martin JH, et al. Trans-spinal focused ultrasound suppresses spinal reflexes in healthy rats [e-pub ahead of print]. Neuromodulation doi:10.1016/j.neurom.2023.04.476, [accessed 07.08.23].
[23] Xu R, O'Reilly MA. Establishing density-dependent longitudinal sound speed in the vertebral lamina. J Acoust Soc Am 2022;151:1516–31.
[24] Xu R, O'Reilly MA. Simulating transvertebral ultrasound propagation with a multi-layered ray acoustics model. Phys Med Biol 2018;63:145017.
[25] Montero AS, Bielle F, Goldwirt L, Lalot A, Bouchoux G, Canney M, et al. Ultrasound-induced blood–spinal cord barrier opening in rabbits. Ultrasound Med Biol 2019;45:2417–26.
[26] Dong F, Shen C, Jiang S, Zhang R, Song P, Yu Y, et al. Measurement of volume-occupying rate of cervical spinal canal and its role in cervical spondylotic myelopathy. Eur Spine J 2013;22:1152–7.
[27] ter Haar G, Coussios C. High intensity focused ultrasound: physical principles and devices. Int J Hyperthermia 2007;23:89–104.
[28] Xu Z, Hall TL, Vlaisavljevich E, Lee Jr. FT. Histotripsy: the first noninvasive, non-ionizing, non-thermal ablation technique based on ultrasound. Int J Hyperthermia 2021;38:561–75.
[29] Finney DJ. Probit analysis: a statistical treatment of the sigmoid response curve. Cambridge: Cambridge University Press; 1952.
[30] Nightingale KR, Church CC, Harris G, Wear KA, Bailey MR, Carson PL, et al. Conditionally increased acoustic pressures in nonfetal diagnostic ultrasound examinations without contrast agents: a preliminary assessment. J Med Ultrasound 2015;34:1–41.
[31] Lee CS, Frizzell LA. Exposure levels for ultrasonic cavitation in the mouse neonate. Ultrasound Med Biol 1988;14:735–42.
[32] Fry WJ, Dunn F. Ultrasonic irradiation of the central nervous system at high sound levels. J Acoust Soc Am 1956;28:129–31.
[33] Frizzell LA, Lee CS, Aschenbach PD, Borrelli MJ, Morimoto RS, Dunn F. Involvement of ultrasonically induced cavitation in the production of hind limb paralysis of the mouse neonate. J Acoust Soc Am 1983;74:1062–5.
[34] Borrelli MJ, Frizzell LA, Dunn F. Ultrasonically induced morphological changes in the mammalian neonatal spinal cord. Ultrasound Med Biol 1986;12:285–95.
[35] Frizzell LA, Chen E, Lee C. Effects of pulsed ultrasound on the mouse neonate: hind limb paralysis and lung hemorrhage. Ultrasound Med Biol 1994;20:53–63.
[36] ThF Hüter, Ballantine Jr HT, Cotter WC. Production of lesions in the central nervous system with focused ultrasound: a study of dosage factors. J Acoust Soc Am 1956;28:192–201.
[37] Ballantine Jr HT, Hueter TF, Nauta WJH, Sosa DM. Focal destruction of nervous tissue by focused ultrasound: biophysical factors influencing its application. J Exp Med 1956;104:337.
[38] Bowsher D. Effect of high-intensity focused ultrasound on nerve cells in spinal cord of mouse. AMA Arch Neurol Psychiatry 1957;78:377–82.
[39] Miller DL, Creim JA, Gies RA. Heating vs. cavitation in the induction of mouse hindlimb paralysis by ultrasound. Ultrasound Med Biol 1999;25:1145–50.
[40] Stolzenberg SJ, Edmonds PD, Torbit CA, Sasmore DP. Toxic effects of ultrasound in mice: damage to central and autonomic nervous systems. Toxicol Appl Pharmacol 1980;53:432–8.
[41] Fry WJ, Fry RB. Temperature changes produced in tissue during ultrasonic irradiation. J Acoust Soc Am 1953;25:6–11.
[42] Taylor KJW. Ultrasonic damage to spinal cord and the synergistic effect of hypoxia. J Pathol 1970;102:41–7.
[43] Taylor KJW, Pond JB. A study of the production of haemorrhagic injury and paraplegia in rat spinal cord by pulsed ultrasound of low megahertz frequencies in the context of the safety for clinical usage. Br J Radiol 1972;45:343–53.
[44] Richards DE, Tyner CF, Shealy CN. Focused ultrasonic spinal commissurotomy: experimental evaluation. J Neurosurg 1966;24:701–7.
[45] Lele PP. Production of deep focal lesions by focused ultrasound-current status. Ultrasonics 1967;5:105–12.
[46] Fry WJ. Action of ultrasound on nerve tissue: a review. J Acoust Soc Am 1953;25:1–5.
[47] Hernandez-Gerez E, Fleming I, Parson SH. A role for spinal cord hypoxia in neurodegeneration. Cell Death Dis 2019;10:861.
[48] Dewhirst M, Viglianti BL, Lora-Michiels M, Hoopes PJ, Hanson MA. Thermal dose requirement for tissue effect: experimental and clinical findings. Proc SPIE Int Soc Opt Eng 2003;4954:37–57.
[49] Meng Y, People CB, Lea-Banks H, Abrahao A, Davidson B, Suppiah S, et al. Safety and efficacy of focused ultrasound induced blood–brain barrier opening, an integrative review of animal and human studies. J Control Release 2019;309:25–36.
[50] Blackmore J, Shrivastava S, Sallet J, Butler CR, Cleveland RO. Ultrasound neuromodulation: a review of results, mechanisms and safety. Ultrasound Med Biol 2019;45:1509–36.
[51] Dunn Francis F, Fry J. Ultrasonic threshold dosages for the mammalian central nervous system. IEEE. Trans Biomed Eng 1971;18:253–6.
[52] Sapareto SA, Dewey WC. Thermal dose determination in cancer therapy. Int J Radiat Oncol Biol Phys 1984;10:787–800.
[53] McDannold N, Vykhodtseva N, Jolesz FA, Hynynen K. MRI investigation of the threshold for thermally induced blood–brain barrier disruption and brain tissue damage in the rabbit brain. Magn Reson Med 2004;51:913–23.
[54] Harris AB, Erickson L, Kendig JH, Mingrino S, Goldring S. Observations on selective brain heating in dogs. J Neurosurg 1962;19:514–21.
[55] Goffinet DR, Choi KY, Brown JM. The combined effects of hyperthermia and ionizing radiation on the adult mouse spinal cord. Radiat Res 1977;72:238–45.
[56] Sminia P, Haveman J, Wondergem J, Van Dltk JDP, Lebesque JV. Effects of 434 MHz microwave hyperthermia applied to the rat in the region of the cervical spinal cord. Int J Hyperthermia 1987;3:441–52.
[57] Sasaki M, Ide C. Demyelination and remyelination in the dorsal funiculus of the rat spinal cord after heat injury. J Neurocytol 1989;18:225–39.
[58] Safety Group of the British Medical Ultrasound Society. Guidelines for the safe use of diagnostic ultrasound equipment. Ultrasound 2010;18:52–9.
[59] U.S. Food and Drug Administration (FDA). Marketing clearance of diagnostic ultrasound systems and transducers. Guidance for Industry and FDA Staff, 2019. Available at: http://resource.nlm.nih.gov/101760255.
[60] National Electrical Manufacturers Association (NEMA). Standard for real-time display of thermal and mechanical acoustic output indices on diagnostic ultrasound equipment. Arlington, VA: NEMA; 2004.
[61] Jago JR, Henderson J, Whittingham TA, Mitchell G. A comparison of AIUM/NEMA thermal indices with calculated temperature rises for a simple third-trimester pregnancy tissue model. Ultrasound Med Biol 1999;25:623–8.
[62] Bigelow TA, Church CC, Sandstrom K, Abbott JG, Ziskin MC, Edmonds PD, et al. The thermal index: its strengths, weaknesses, and proposed improvements. J Med Ultrasound 2011;30:714–34.
[63] Carstensen EL, Law WK, McKay ND, Muir TG. Demonstration of nonlinear acoustical effects at biomedical frequencies and intensities. Ultrasound Med Biol 1980;6:359–68.
[64] Kim HA, Han JM. The effect of ultrasound irradiation on the neural cell adhesion molecules (NCAM) expression in rat spinal cord after the sciatic nerve crush injury. J Korean Phys Ther 2007;19:41–55.
[65] Guadallini Jatte F, Mazzer N, Vilela Monte-Raso V, Leite Leoni AS, Barbieri CH. Therapeutic ultrasound on the spinal cord accelerates regeneration of the sciatic nerve in rats. Acta Ortop Bras 2011;19:213.
[66] Hong YR, Lee EH, Park KS, Han M, Kim KT, Park J. Ultrasound stimulation improves inflammatory resolution, neuroprotection, and functional recovery after spinal cord injury. Sci Rep 2022;12:3636.
[67] Ahmed RU, Alam M, Li S, Palanisamy P, Zhong H, Zheng YP. A novel therapeutic approach of ultrasound stimulation to restore forelimb functions following cervical cord injury in rats. J Neurorestoratol 2023;11:100067.
[68] Zhang F, He X, Dong K, Yang L, Ma B, Liu Y, et al. Combination therapy with ultrasound and 2D nanomaterials promotes recovery after spinal cord injury via piezo1 downregulation. J Nanobiotechnol 2023;21:91.
[69] Liao YH, Wang B, Chen MX, Liu Y, Ao LJ. LIFU alleviates neuropathic pain by improving the KCC_2 expression and inhibiting the CAMKIV-KCC_2 pathway in the L_4–L_5 section of the spinal cord. Neural Plast 2021;2021:6659668.
[70] Zannou AL, Khadka N, FallahRad M, Truong DQ, Kopell BH, Bikson M. Tissue temperature increases by a 10 kHz spinal cord stimulation system: phantom and bioheat model. Neuromodulation 2021;24:1327–35.
[71] Guieu JD, Hardy JD. Effects of heating and cooling of the spinal cord on preoptic unit activity. J Appl Physiol 1970;29:675–83.
[72] Chai CY, Lin MT. Effects of heating and cooling the spinal cord and medulla oblongata on thermoregulation in monkeys. Physiol J 1972;225:297–308.
[73] Boulant JA, Hardy JD. The effect of spinal and skin temperatures on the firing rate and thermosensitivity of preoptic neurones. Physiol J 1974;240:639.
[74] Madden CJ, Morrison SF. Central nervous system circuits that control body temperature. Neurosci Lett 2019;696:225–32.
[75] Racinais S, Gaoua N, Grantham J. Hyperthermia impairs short-term memory and peripheral motor drive transmission. J Physiol 2008;586:4751–62.
[76] Hoffman BU, Baba Y, Lee SA, Tong CK, Konofagou EE, Lumpkin EA. Focused ultrasound excites action potentials in mammalian peripheral neurons in part through the mechanically gated ion channel piezo2. Proc Natl Acad Sci USA 2022;119:e2115821119.
[77] Yoo S, Mittelstein DR, Hurt RC, Lacroix J, Shapiro MG. Focused ultrasound excites cortical neurons via mechanosensitive calcium accumulation and ion channel amplification. Nat Commun 2022;13:493.
[78] Zheng W, Nikolaev YA, Gracheva EO, Bagriantsev SN. Piezo2 integrates mechanical and thermal cues in vertebrate mechanoreceptors. Proc Natl Acad Sci USA 2019;116:17547–55.
[79] Wijerathne TD, Ozkan AD, Lacroix JL. Yoda1s energetic footprint on piezo1 channels and its modulation by voltage and temperature. Proc Natl Acad Sci USA 2022;119:e2202269119.
[80] Hynynen K, McDannold N, Vykhodtseva N, Jolesz FA. Noninvasive MR imaging-guided focal opening of the blood–brain barrier in rabbits. Radiology 2001;220:640–6.

[81] McDannold N, Vykhodtseva N, Hynynen K. Blood–brain barrier disruption induced by focused ultrasound and circulating preformed microbubbles appears to be characterized by the mechanical index. Ultrasound Med Biol 2008;34:834–40.
[82] McMahon D, Hynynen K. Acute inflammatory response following increased blood–brain barrier permeability induced by focused ultrasound is dependent on microbubble dose. Theranostics 2017;7:3989.
[83] Song KH, Fan AC, Hinkle JJ, Newman J, Borden MA, Harvey BK. Microbubble gas volume: a unifying dose parameter in blood–brain barrier opening by focused ultrasound. Theranostics 2017;7:144.
[84] McMahon D, O'Reilly MA, Hynynen K. Therapeutic agent delivery across the blood–brain barrier using focused ultrasound. Annu Rev Biomed Eng 2021;23:89113.
[85] O'Reilly MA, Hynynen K. Blood–brain barrier: real-time feedback-controlled focused ultrasound disruption by using an acoustic emissions-based controller. Radiology 2012;263:96.
[86] Fletcher SMP, O'Reilly MA. Analysis of multifrequency and phase keying strategies for focusing ultrasound to the human vertebral canal. IEEE Trans Ultrason Ferroelectr Freq Control 2018;65:2322–31.
[87] Fletcher SMP, Choi M, Ramesh R, O'Reilly MA. Focused ultrasound-induced blood–spinal cord barrier opening using short-burst phase-keying exposures in rats: a parameter study. Ultrasound Med Biol 2021;47:1747–60.
[88] Wachsmuth J, Chopra R, Hynynen K. Feasibility of transient image-guided blood–spinal cord barrier disruption. AIP Conf Proc 2009;1113:256–9.
[89] Fletcher SMP, Ogrodnik N, O'Reilly MA. Enhanced detection of bubble emissions through the intact spine for monitoring ultrasound-mediated blood–spinal cord barrier opening. IEEE Trans Biomed Eng 2019;67:1387–96.
[90] Fletcher SMP, Choi M, Ogrodnik N, O'Reilly MA. A porcine model of transvertebral ultrasound and microbubble-mediated blood–spinal cord barrier opening. Theranostics 2020;10:7758.
[91] Payne AH, Hawryluk GW, Anzai Y, Odeen H, Ostlie MA, Reichert EC, et al. Magnetic resonance imaging-guided focused ultrasound to increase localized blood–spinal cord barrier permeability. Neural Regen Res 2017;12:2045.
[92] Cross CG, Payne AH, Hawryluk GW, Haag-Roeger R, Cheeniyil R, Brady D, et al. Quantification of blood–spinal cord barrier permeability after application of magnetic resonance-guided focused ultrasound in spinal cord injury. Med Phys 2021;48:4395–401.
[93] Bhimreddy M, Routkevitch D, Hersh AM, Mohammadabadi A, Menta AK, Jiang K, et al. Disruption of the blood–spinal cord barrier using low-intensity focused ultrasound in a rat model. J Vis Exp 2023;193:e65113.
[94] Ando T, Sato S, Toyooka T, Uozumi Y, Nawashiro H, Ashida H, et al. Site-specific gene transfer into the rat spinal cord by photomechanical waves. J Biomed Opt 2011;16:108002.
[95] Frizado AP, O'Reilly MA. A numerical investigation of passive acoustic mapping for monitoring bubble-mediated focused ultrasound treatment of the spinal cord. J Acoust Soc Am 2023;153:2271–84.
[96] ter Haar G, Shaw A, Pye S, Ward B, Bottomley F, Nolan R, et al. Guidance on reporting ultrasound exposure conditions for bio-effects studies. Ultrasound Med Biol 2011;37:177–83.
[97] Padilla F, Ter Haar G. Recommendations for reporting therapeutic ultrasound treatment parameters. Ultrasound Med Biol 2022;48:1299–308.
[98] Baron C, Aubry JF, Tanter M, Meairs S, Fink M. Simulation of intracranial acoustic fields in clinical trials of sonothrombolysis. Ultrasound Med Biol 2009;35:1148–58.
[99] Xu X, O'Reilly MA. A spine-specific phased array for transvertebral ultrasound therapy: design and simulation. IEEE Trans Biomed Eng 2019;67:256–67.
[100] Sanford D. MSc thesis. Northridge, CA: California State University; 2020.
[101] Adams C, Jones RM, Yang SD, Kan WM, Leung K, Zhou Y, et al. Implementation of a skull-conformal phased array for transcranial focused ultrasound therapy. IEEE Trans Biomed Eng 2021;68:3457–68.
[102] Maimbourg G, Houdouin A, Deffieux T, Tanter M, Aubry JF. 3D-Printed adaptive acoustic lens as a disruptive technology for transcranial ultrasound therapy using single-element transducers. Phys Med Biol 2018;63:025026.
[103] Jimenez-Gambin S, Jimenez N, Benlloch JM, Camarena F. Holograms to focus arbitrary ultrasonic fields through the skull. Phys Rev Appl 2019;12:014016.
[104] Xu R, Martin D, O'Reilly MA. Array-based beamforming to the vertebral canal: demonstration of feasibility. Proc IEEE Int Ultrason Symp 2021:1–4.
[105] Qiao S, Elbes D, Boubriak OA, Urban JPG, Coussios CC, Cleveland RO. Delivering focused ultrasound to intervertebral discs using time-reversal. Ultrasound Med Biol 2019;45:2405–16.
[106] Adams MS, Lotz JC, Diederich CJ. In silico feasibility assessment of extracorporeal delivery of low-intensity pulsed ultrasound to intervertebral discs within the lumbar spine. Phys Med Biol 2020;65:215011.
[107] Scott SJ, Salgaonkar V, Prakash P, Burdette EC, Diederich CJ. Interstitial ultrasound ablation of vertebral and paraspinal tumours: parametric and patient-specific simulations. Int J Hyperthermia 2014;30:228–44.
[108] Fugate RQ, Fried DL, Ameer GA, Boeke BR, Browne SL, Roberts PH, et al. Measurement of atmospheric wavefront distortion using scattered light from a laser guidestar. Nature 1991;353:144–6.
[109] Gateau J, Marsac L, Pernot M, Aubry JF, Tanter M, Fink M. Transcranial ultrasonic therapy based on time reversal of acoustically induced cavitation bubble signature. IEEE Trans Biomed Eng 2009;57:134–44.
[110] Jones RM, Huang Y, Meng Y, Scantlebury N, Schwartz ML, Lipsman N, et al. Echo-focusing in transcranial focused ultrasound thalamotomy for essential tremor: A feasibility study. Mov Disord 2020;35:2327–33.
[111] Clement GT, Hynynen K. A non-invasive method for focusing ultrasound through the human skull. Phys Med Biol 2002;47:1219.
[112] Aubry JF, Tanter M, Pernot M, Thomas JL, Fink M. Experimental demonstration of noninvasive transskull adaptive focusing based on prior computed tomography scans. J Acoust Soc Am 2003;113:84–93.
[113] Aubry JF, Bates O, Boehm C, Butts Pauly K, Christensen D, Cueto C, et al. Benchmark problems for transcranial ultrasound simulation: intercomparison of compressional wave models. J Acoust Soc Am 2022;152:1003–19.
[114] Olinger C, Vest J, Tarasek M, Yeo D, DiMarzio M, Burdette C, et al. MR thermometry imaging for low intensity focused ultrasound modulation of spinal nervous tissue. Magn Reson Imaging 2023;101:35–9.
[115] Singh S, Tetreault L, Kalsi-Ryan S, Nouri A, Fehlings MG. Global prevalence and incidence of traumatic spinal cord injury. J Clin Epidemiol 2014;6:309–31.
[116] Ning GZ, Song WY, Xu H, Zhu RS, Wu QL, Wu Y, et al. Bone marrow mesenchymal stem cells stimulated with low-intensity pulsed ultrasound: better choice of transplantation treatment for spinal cord injury: treatment for SCI by LIPUS-BMSCS transplantation. CNS Neurosci Ther 2019;25:496–508.
[117] Arbab M, Matuszek Z, Kray KM, Du A, Newby GA, Blatnik AJ, et al. Base editing rescue of spinal muscular atrophy in cells and in mice. Science 2023;380:eadg6518.
[118] Persson J, Stromqvist B, Zanoli G, McCarthy I, Lidgren L. Ultrasound nucleolysis: an in vitro study. Ultrasound Med Biol 2002;28:1189–97.
[119] Nau WH, Diederich CJ, Shu R. Feasibility of using interstitial ultrasound for intradiscal thermal therapy: a study in human cadaver lumbar discs. Phys Med Biol 2005;50:2807.
[120] Bass EC, Nau WH, Diederich CJ, Liebenberg E, Shu R, Pellegrino R, et al. Intradiscal thermal therapy does not stimulate biologic remodeling in an in vivo sheep model. Spine 2006;31:139–45.
[121] Nau WH, Diederich CJ, Shu R, Kinsey A, Bass E, Lotz J, et al. Intradiscal thermal therapy using interstitial ultrasound: an in vivo Investigation in ovine cervical spine. Spine 2007;32:503–11.
[122] Horne DA, Jones PD, Adams MS, Lotz JC, Diederich CJ. LIPUS far-field exposimetry system for uniform stimulation of tissues in-vitro: development and validation with bovine intervertebral disc cells. Biomed Phys Eng Express 2020;6:035033.
[123] Weeks EM, Platt MW, Gedroyc W. MRI-guided focused ultrasound (MRGFUS) to treat facet joint osteoarthritis low back pain: case series of an innovative new technique. Eur Radiol 2012;22:2822–35.
[124] Harnof S, Zibly Z, Shay L, Dogadkin O, Hanannel A, Inbar Y, et al. Magnetic resonance-guided focused ultrasound treatment of facet joint pain: summary of preclinical phase. J Ther Ultrasound 2014;2:1–10.
[125] Zhang W, Trivedi H, Adams M, Losey AD, Diederich CJ, Ozhinsky E, et al. Anatomic thermochromic tissue-mimicking phantom of the lumbar spine for pre-clinical evaluation of MR-guided focused ultrasound (MRGFUS) ablation of the facet joint. Int J Hyperthermia 2021;38:130–5.
[126] Tiegs-Heiden CA, Hesley GK, Long Z, Lu A, Lamer TJ, Gorny KR, et al. MRI-Guided focused ultrasound ablation of painful lumbar facet joints: a retrospective assessment of safety and tolerability in human subjects. Pain Med 2023;24:1219–23.
[127] Kaye EA, Monette S, Srimathveeravalli G, Maybody M, Solomon SB, Gulati A. MRI-Guided focused ultrasound ablation of lumbar medial branch nerve: feasibility and safety study in a swine model. Int J Hyperthermia 2016;32:786–94.
[128] Hellman A, Maietta T, Byraju K, Park YL, Liss A, Prabhala T, et al. Effects of external low intensity focused ultrasound on electrophysiological changes in vivo in a rodent model of common peroneal nerve injury. Neuroscience 2020;429:264–72.
[129] Chen J, LeBlang S, Hananel A, Aginsky R, Perez J, Gofeld M, et al. An incoherent HIFU transducer for treatment of the medial branch nerve: mumerical study and in vivo validation. Int J Hyperthermia 2020;37:1219–28.
[130] Hellman A, Maietta T, Clum A, Byraju K, Raviv N, Staudt MD, et al. Pilot study on the effects of low intensity focused ultrasound in a swine model of neuropathic pain [e-pub ahead of print]. J Neurosurg doi:10.3171/2020.9.JNS202962 [accessed 21.02.23]
[131] Li S, Alam M, Ahmed RU, Zhong H, Wang XY, Ng S, et al. Ultrasound-driven piezoelectric current activates spinal cord neurocircuits and restores locomotion in rats with spinal cord injury. Bioelectron Med 2020;6:1–9.
[132] Ebadi E, Henschke N, Forogh B, Ansari NN, van Tulder MW, Babaei-Ghazani A, et al. Therapeutic ultrasound for chronic low back pain. Cochrane Database Syst Rev 2020;7:CD009169.
[133] Gnatz SM. Increased radicular pain due to therapeutic ultrasound applied to the back. Arch Phys Med Rehabil 1989;70:493–4.
[134] Ebadi S, Ansari NN, Naghdi S, Jalaei S, Sadat M, Bagheri H, et al. The effect of continuous ultrasound on chronic non-specific low back pain: a single blind placebo-controlled randomized trial. BMC. Musculoskelet Disord 2012;13:1–10.
[135] Sciubba DM, Burdette EC, Cheng JJ, Pennant WA, Noggle JC, Petteys RJ, et al. Percutaneous computed tomography fluoroscopy-guided conformal ultrasonic ablation of vertebral tumors in a rabbit tumor model. J Neurosurg Spine 2010;13:733–79.
[136] Curry DM, Beaton GH. Effects of destruction of the thoracic spinal cord on spermatogenesis in the mouse. Endocrinology 1958;63:254–6.
[137] Lele PP. Effects of focused ultrasonic radiation on peripheral nerve, with observations on local heating. Exp Neurol 1963;8:47–83.
[138] Takagi SF, Higashino S, Shibuya T, Osawa N. The actions of ultrasound on the myelinated nerve, the spinal cord and the brain. Jpn J Physiol 1960;10:183–93.
[139] Liao YH, Chen MX, Chen SC, Luo KX, Wang B, Ao LJ, et al. Low-intensity focused ultrasound alleviates spasticity and increases expression of the neuronal K-Cl cotransporter in the L_4–L_5 sections of rats following spinal cord injury. Front Cell Neurosci 2022;16:882127.
[140] Wang B, Zhao H, Chen M, Chen S, Liao Y, Tang X, et al. Proteomics reveals the effect of low-intensity focused ultrasound on spasticity after spinal cord injury. Turk Neurosurg 2023;33:77–86.
[141] Oakden W, Kwiecien JM, O'Reilly MA, Lake EMR, Akens MK, Aubert I, et al. A non-surgical model of cervical spinal cord injury induced with focused ultrasound and microbubbles. J Neurosci Methods 2014;235:92–100.
[142] Oakden W, Kwiecien JM, O'Reilly MA, Dabrowski W, Whyne C, Finkelstein J, et al. Quantitative MRI in a non-surgical model of cervical spinal cord injury. NMR Biomed 2015;28:925–36.